OPTIMIZATION OF THE FILARDO PUMP: A NOVEL, ROBUST, SUSTAINABLE AND LOW COST SELF-POWERED WATER PUMP FOR USE IN FREE-FLOWING STREAMS

A Thesis

Presented to the Faculty of the Graduate School

of Cornell University

in Partial Fulfillment of the Requirements for the Degree of

Master of Science

by

Diego Fernando Muriel Delgado

August 2013

ABSTRACT

The design of infrastructure to supply water depends on local conditions including geophysical features, available technology, traditions and culture, as well as the availability of local human and economic resources. The costs for designing, building, maintaining, monitoring, and replacing the required infrastructure for water supply can rapidly escalate when any of the above factors is inadequate or insufficient. Furthermore, effects of global climate change increase the risk associated to the existing infrastructure, calling for more robust, flexible, and adaptable technologies to satisfy water demand. We present the design and optimization for a low-cost, robust, sustainable, water-powered pump that addresses these challenges and has many advantages over existing technologies: it requires no external energy source; it is immersed in a free-flowing, unaltered body of water; it can operate in shallow water, low flow, and low-head conditions; it has low cost and low weight relative to the work performed; and it can be made small for households or scaled up for industrial applications. We show how the proposed technology, based on a permanent but unstable sinusoidal deformation composed of two oscillating plastic sheets, lifts water over the energy grade line of the fluid in which it is immersed, and we optimize the performance by scaling its geometrical aspects (thickness, width, and space between polypropylene sheets) and by designing parts involved in its operation (dowel rods for transversal reinforcement, internal membrane and outlet connection, length and tension of strings inducing the deformation, and check valve). In addition, this technology presents an opportunity for low-cost, sustainable water supply for households, agricultural and industrial applications

everywhere, not just in the rural developing world.

BIOGRAPHICAL SKETCH

The author was born in Cali, Colombia, in 1985. He graduated from Universidad Javeriana Cali, as a Civil Engineer in 2008. After spending three years in research on the hydrodynamics of Potable Water Storage Tanks and Chlorine Contact tanks, he moved in 2011 to Ithaca, NY, to pursue his graduate studies at Cornell University, working the first year with Professor Philip Liu studying the scaling factors of a device for wave energy extraction, and later joining the project of optimization of a novel self-powered lifting device, which has been the basis for this document.

To Nora and Ana

ACKNOWLEDGEMENTS

Sincere thanks go to Edwin Cowen for his valuable advice and guidance in this project. Special thanks go to Pietro Filardo for letting his idea to be the topic of study in this research. To Rafael Tinoco for his support, guidance and encouragement during the early stages of the study. Thanks to Blair Johnson, Erika Johnson, Seth Schweitzer and Nimish Pujara for sharing their knowledge of facilities and equipment at the DeFrees Hydraulic Laboratory.

Acknowledgement must go to the Fulbright Program for funding the author's studies at Cornell University. Special thanks go to the Fulbright Colombian Commission and LASPAU for their support and guidance during the studies. Special thanks to the Atkinson Center for a Sustainable future, who's Rapid Response Fund grant allowed the purchase of materials used in this research. Any opinions and comments are those of the author and do not necessarily reflect the views of the sponsors.

CONTENTS

LIST OF FIGURES

LIST OF TABLES

LIST OF SYMBOLS

- δ : separation between ribbons
- $\eta_{(t)}$: instantaneous measurements of distance
- H : flow depths
- h : water lift
- K_m : minor loss coefficient defined as
- l : strings length
- $\triangle P_{(t)}$: pressure differences
- S_{aa} : power spectral density (PSD) function
- $u_{(t)}$: instantaneous measurements of longitudinal velocity
- U_0 : upstream flow velocity
- $v_{(t)}$: instantaneous measurements of lateral velocity
- $w_{(t)}$: instantaneous measurements of vertical velocity
- W_r : separation between side bars
- W : width of the ribbons

CHAPTER 1

INTRODUCTION

1.1 Objectives

After the Millennium Summit in 2000 and the approval of the Millennium Declaration, the objective of improving water and sanitation sectors has played an important role in the political agenda of many countries. The goal of achieving environmental sustainability established a target that by 2015 the population without access to safe drinking water and sanitation should be reduced by half. According to the United Nations [24] 11% of the global population—783 million people—remains without access to an improved source of drinking water; with the current trends, 605 million people will still lack coverage in 2015. They also say that coverage with improved drinking water sources for rural populations is still a concern. In 2010, 96% of the urban population had access to improved drinking water, compared with 81% of the rural population. Additionally, the World Health Organization (WHO) and UNICEF [23] declared, based on 1990-2011 data, that 83% of the population without access to an improved drinking water source lived in rural areas.

In addition to these statistics, another concern comes from the definition of the term “drinking water" or "safe water". According to the International Bank for Reconstruction and Development [29], access to drinking water from an improved source does not ensure that the water is safe or adequate, as these characteristics are not tested at the time of survey. They affirmed that even if information on access to an improved water source is widely used, its level of improvement varies widely, and in consequence the clasification of a water source based on quality is extremely subjective. Also, they claim that terms such as "safe," "improved," "adequate," and "reasonable" may have different meanings in different countries despite official WHO definitions.

This problem is seen in many developing countries, when the authorities try to improve statistics when evaluating the performance of the government. For example, in Colombia it is very common to see the use of the phrases "access to aqueducts," "access to water supply," or "access to safe water" with no further explanation of the terms. While *access to aqueducts* could mean access to piped water, there is no regard for the state of the infrastructure or the quality of the water supplied, which could be either treated or untreated. *Access to water supply* could mean that a river is nearby, or that the household has a way to store rain water. In some cases, *access to safe water* could refer to either of the first two terms explained. With this in mind, the Colombian National Department of Statistics [5] reported in 1993 that 94.6% of the urban population had access to aqueducts, and 41.4% of the rural population had access to a water supply. For Colombia it was clear that the lag in rural communities' access was important, and after the Millennium Summit the first official statistic was an increase in reported access to safe water to 66% of the rural households by 2003 [6]. From the National Department of Statistics in Colombia[7] it was inferred that some of the challenges to increasing the penetration of water service is the low density of the households in the rural settlements in Colombia, the difficult access to those communities, particularly in the Pacific region, due to the lack of proper roads, dense forests, and public turmoil, and weak public policies used in many rural locations that leave these communities with a weak regional planning program. In the same way, similar problems can be seen in rural communities of other developing countries.

In general, the infrastructure designed for water supply is affected by local conditions, traditions and culture, the availability of human and financial resources, and of course the efficiency of the technology itself. The expected design, maintenance and monitoring costs will grow rapidly if any of these factors is inadequate or insufficient. If in addition to this the possibility of extreme events caused by climate change adds to, the risk to existing infrastructure increases further. Therefore there is a significant and immediate need for a flexible, low cost and robust technology to meet current water demand. The aim of this work is to study and develop a highly novel pump technology invented by B. Pietro Filardo of the U.S. company Pliant Energy System, LLC. The Filardo pump has the potential to meet the challenges outlined above since it:

- Does not require an external power source.
- Can operate in extreme conditions such as shallow water levels, debris-laden flows, or low flows.
- Is low cost due to the absence of articulating components, bearings, low weight in relation to work performed and compared with other existing solutions, enabling scalability.
- Is low Maintenance: requiring only occasional cleaning.
- Operates almost silently, gentle interaction with plant and animal life, and harmless to humans.
- Posesses excellent resistance to extreme flow events such as during a flood.
- And finally, this pump can be implemented in rural areas away from sources of water, replacing the work of women and children who must walk every day carrying buckets of water to their homes, increasing qual-

ity of life, gender equity and productivity of households and the community.

The *general objective* of this thesis is to determine optimal configurations of the Filardo pump in terms of what is the optimal size and spacing of the primary ribbon membranes and the position and tension in their support and mounting interfaces which achieves maximum conversion of river kinetic energy to pump head and delivered flow rate.

1.2 Current technologies for energy extraction on free stream flows

As explained in Cowen et al. [3] and Cowen et al. [4], water lifting mechanisms can be classified by either the water source in use, the technology implemented in the mechanism, or by the power source required to operate them [1]. Available water sources are ground water, surface water, and rain water. Water lifting technologies include: rope and bucket (loose, through a pulley, or on a windlass); bucket pump; rope pump; suction plunger hand-pump; direct action pump; deep-well piston pump; deep-well diaphragm pump; centrifugal pump; electrical submersible pump; axial flow pump; and hydraulic ram. And power sources are: human power; animal traction; wind driven; photovoltaic systems; electrical, petrol or diesel engines; and self-water powered. A comprehensive description is reported by Fraenkel [11] and updated by Fraenkel and Thake [12], and from these references it is clear that there is no technology capable of solving the water crisis in rural communities currently.

According to Fraenkel [11] the cost of human labor required in water lifting human power devices is considerable and even more expensive than technologies shuch as solar photovoltaic panels. Additionally, maintenance problems affect the availability of already installed devices [14]. In an attempt to address these disadvantages, variations of rope and washer pump [28], treadle pumps [16], and flow reciprocating pumps [2] have been developed. Still, these variations require special machinery and parts for maintenance and repair, affecting their sustainability.

Meanwhile, solar power mechanisms suffer either from high cost per kW capacity installed, or the use of relatively sophisticated and often fragile mechanical components. First, the cost of traditional pumps powered by photovoltaic systems (PV) comes from the necessity of conversion of energy from light to electricity to mechanical force, which requires the coupling of the PV system with an existing lifting mechanism. Second, the reliability and complexity of solar thermal pumps (traditional pumps driven by closed cycle heat-engines) comes from the sophistication of the components used and the fragility of solar collectors.

In the same way as with solar power, wind power mechanisms must be divided into those powered by wind-generated electricity, and those mechanical wind pumps using mechanical energy from the wind to transport water [17, 20]. Regardless of the type, wind powered pumps are highly efficient in converting harvested energy into useful work, require low maintenance and can operate in a wide wind speed range. However, the main disadvantages are the high initial capital cost, the size, skills required for assembly, intermittency of the wind resource, and maintenance costs [26].

In the area of self-water-powered devices, waterwheels like the Noria are limited in the lifting height by their own radii. On the contrary the Spiral waterwheel pump can lift water to a height several times its diameter. For both devices the only precise machined components are the bearings, and additionally for the latter the rotating coupling that connects the pipe exiting the hub of the device to the outlet pipe. Some of the disadvantages are the initial capital cost, strong foundations required, and vulnerability to flood events. On the other hand, a comparatively simple mechanism is the Ram pump. This device requires precision machined parts, a supply of water under pressure, meaning a head differential and sealed penstock. Additionally, the coil pump and its commercial adaptation, the sling pump, operate under the same concept of self powered devices. The coil pump is in principle the Archimedes screw operating in a horizontal plane with a coiled pipe, and the sling pump includes the addition of a propeller. Both devices require sufficient water depth to submerge the mechanism and enough current to power them. Both designs are also limited in the lifting head and the flow rate delivered. Finally, a review of current patents shows a diverse range of water powered pumps. In general, all devices are characterized by requiring costly machined parts [3, 4].

1.3 The Filardo Pump Concept

Fig. 1.1 presents an adaptation of drawings of the Filardo Pump concept. The general idea is to use elastic materials to harness river kinetic energy and to convert this energy into water pumped. On the *left* of the figure we can see in the upper part two elastic materials with a membrane in the middle. By applying an external force we can see in the lower part that a deformation is induced and

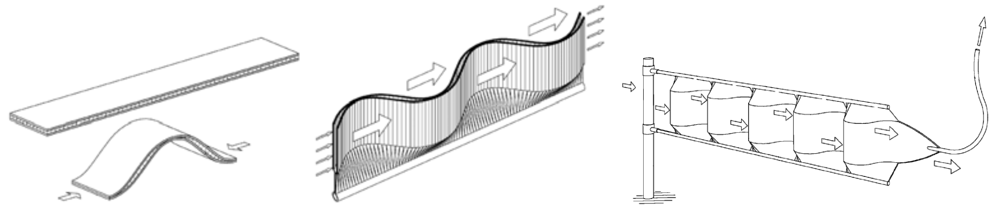

Figure 1.1: The Filardo concept of pliant elements for harnessing forces of moving fluids: Elastic material coupling and deformation (*left*); mounting and strings (*middle*); general mounting for deployment (*right*). Drawings adapted from [10].

three pinching points are created (two in the edges of the ribbons and one in the crest of the deformation). This external forced applied is permanent, and so is the deformation, locking potential energy into the prototype. In the *middle* of the figure we can observe the plastic sheets (called ribbons) already mounted and deformed. In principle, this deformation is permanent and unstable, allowing the ribbon to oscillate once it is placed in moving water. With these oscillations, the pinching points travel in the direction of the flow, and if an outlet pipe is inserted in the design (*right*) and a check-valve added, water will be pumped without the need of external energy other than that provided by the flowing stream. A detailed description of the concept is presented in Filardo [10].

Additionally to the concept, Pliant Energy Systems provided the initial theory of operation and the first physical model composed by a single ribbon of 30cm by 60cm. The information from this initial prototype helped on building the subsequent prototypes of this thesis. Pliant studied the coefficient of drag experienced by a single ribbon [21] and a series of pump configurations (two ribbons and a membrane) based on ABAQUS software [22]. Both of these reports were also a starting point for the devices built in this study.

	Wind	Solar PV Electric	Solar Thermal	Noria Wheel	Sling/Spiral	Ribbon Pump	Combustion/Electric	Ram	Human/Animal
Robust	✓	-	-	✗	✗	✓	✓	✓	-
Very Shallow Water	✓	✓	✓	✗	✗	✓	✓	✓	✓
Human/animal safety	✓	✓	-	✗	-	✓	-	✓	✓
Low fab cost	✗	✗	✗	✗	-	✓	✗	✓	✓
Low install cost	✗	✓	✗	✗	✓	✓	✓	✗	-
Low operate/maintenance cost	-	✓	-	✓	✓	✓	✗	✓	✗
Low environmental cost	✓	✓	✓	✓	✓	✓	✗	✓	-
Operates under surface ice	✓	✓	✓	✗	✗	✓	✓	-	-
24 hour operation	✓	✗	✗	✓	✓	✓	✓	✓	✓
Independent of weather	✗	✗	✗	✓	✓	✓	✓	✗	✓

Figure 1.2: Comparison of the capabilities of various pump technologies .

1.4 A comparison of capabilities between the Filardo Pump and current competitors

There are a number of different devices proposed to solve the requirements of water delivery either for human consumption or irrigation in rural communities. If we consider different aspects as robustness, the cost of fabrication and installation, the operation and maintenance costs, the environmental cost among other characteristics, there is no single mechanism that faces all the challenges at once except for the device studied in this research (Figure 1.2). Apart from the Filardo Pump, there must be a trade off when implementing other lifting device. For example, in order to obtain robustness and low environmental costs in wind, solar and thermal systems we need to sacrifice the fabrication cost, and several times the cost related to installing these systems. On the contrary, the Filardo pump is robust enough to operate under variable flow conditions and it has a low cost of fabrication and installation. In the same way, it does not require high maintenance and it does not involve costly materials or precision machined parts.

As we will see later in this document, the shut-off head of the Filardo pump is still to be determined, and the results for the flow rate delivered at specific heads it is also at an early stage. From [3] the maximum flow rate for the original design is $1m^3/h$ at a maximum head of $3m$. The results that will be presented in this research will showed a maximum flow rate of $30L/h$. First, it is important to highlight that even though it is a low flow rate compare to the competitors (variable for Noria and Spiral water wheel pumps; 2 to 10 m^3/h for coil and slinging pumps; and variable for the ram pump) it is an exciting result at these early stages. Second, it is important to mention that this flow rate is already enough to supply the expected optimal daily human water consumption for a household ($100L/day$ for an average person, [15]).

1.5 Mechanics of motion of flexible plates immersed in free stream flows

Based on the literature review, there is no similar device transforming fluid kinetic energy into work performed to lift water. Similar oscillations are reported and quantified in flags [30] but the reported vibration was only constrained in one point. In similar ways Zang et al. [30] report the complexity of the interaction of flexible and deformable shapes with surrounding fluids. No study has quantified the interaction of two flexible plates with their movement constrained in multiple points with an induced sinusoidal deformation.

1.6 Outline

We focus this document in the optimization of the Filardo pump by changing a range of parameters in the original design and by understanding their relationship with the frequency of oscillation and the volume of water pumped at a certain height. Chapter 2 presents the methodology used in the research and the tools for data analysis. Chapter 3 details the prototypes built and the experiments run in each of the prototypes, explaining which parameter was changed and the reasons for changing it. Chapter 4 discusses the results of all tests and analyzes the performance of the self-powered pump based on these results. Chapter 5 presents the conclusions of this research and recommendations for future work.

CHAPTER 2

METHODOLOGY

In order to demonstrate and optimize the Filardo Pump concept a series of prototypes were developed and built. The initial design came from one single elastic material termed in this document a *ribbon*. The pump itself is formed by two of these plastic sheets held closely together under the deformation provided by a series of strings attached to a frame. For each prototype the flow-rate pumped was determine as well as the frequency of oscillations in each test case. The prototyping process involved the change of the following aspects: 1) transversal reinforcement, 2) outlet configuration, 3) internal membrane, 4) check valve, 5) outlet pipe, 6) spacing between ribbons, 7) thickness of the ribbons, and 8) width of ribbons.

All of the experiments were conducted in a flume with different prototypes of the self-powered pump. An aluminum frame with variable width was used to hold the prototypes in place as well as to induce the sine-wave in the plastic membranes by means of tension. Water velocity and the oscillation of the ribbons were measured with an Acoustic Doppler Velocimeter (ADV). This chapter will present a description of the facilities and equipment used, an explanation of the tools for data analysis and data quality control, and it will finish with a description of the prototypes.

2.1 Experimental measurements

Experiments were conducted in a 8.0m long, 0.60m wide recirculating type open channel flume with glass sidewalls and Super Abrasion Resistant acrylic bed in the DeFrees Hydraulics Laboratory in the School of Civil and Environmental Engineering at Cornell University. The flow rates for each experiment were driven by two variable frequency controlled centrifugal pumps.

The upstream flow velocity, U_0, was defined as the velocity measured on the centerline of the flume at the highest distance above the bed, where the ADV measurements were not affected by surface effects. Also, in order to avoid the aluminum frame from affecting the measurement of U_0, the ADV was located $2.0m$ upstream from the beginning of the frame. In the same way, three flow depths ($H = 30.0cm$, $H = 32.5cm$ and $H = 37.0cm$) were used to test that surface effects would not affect or influence the ribbon oscillations. The coordinate system was defined with x in the streamwise direction, y cross-stream, and z vertical (depth) to the bed. A Nortek Vectrino ADV with firmware was used for velocity measurements at different locations. The same ADV, running in Distance-Check mode, was used to calculate amplitudes and frequencies of the ribbon oscillations. For all of the measurements the transmit length was set to $1.8mm$ and the sampling volume to $7.0mm$. For the experiment series from $T01$ to $T03$, 2^{14} samples at a rate of $200Hz$ were taken for velocity measurements and 2^{11} samples at a rate of $10Hz$ for distance and frequency measurements, for the remaining series ($T04$) 2^{15} samples at a rate of $200Hz$ were taken for velocity measurements. The ADV was mounted on a movable steel platform above the flume that allowed manual positioning of the ADV in all three directions.

The head loss coefficients through check valves was measured with two different pressure sensors to provide differential pressure loss: $7kPa$ and $2inH_2O$. The first one, OMEGA's PX26-001DV series pressure sensors is a PC mountable wet/wet differential pressure sensor with a maximum voltage of $16.7mV$ and a corresponding value of $7kPa$. The second one is a low range wet/wet differential pressure transducer by Omegadyne, Inc. with a maximum voltage of $5V$ and a corresponding value of $2inH_2O$. Each data point is reported based on a record length of 10,000 samples at $100Hz$.

The lifting head h is defined as the height measured from the still water surface level of the flume to the lower inner edge of the outlet pipe. The prototypes were tested from 5 to 25 cm of lifting head. On the other hand, the flow rate delivered was measured by collecting a volume of water in a certain period of time for all combinations of lifting heads and average flume speeds.

2.2 Data processing and analysis

The ADV collected instantaneous measurements of longitudinal ($u(t)$), lateral ($v(t)$), and vertical ($w(t)$) velocity components, both for mean flow stream velocities and for single point records measured above the ribbon. The ADV also collected instantaneous distance ($\eta(t)$) to the ribbon relatively to an arbitrary datum when it was placed above the ribbon. The pressure sensors gathered instantaneous pressure differences ($\triangle P(t)$). All of this data was processed using $MatLab^{®}$, version 2012b.

For all data records a Fourier Analysis was performed to understand the frequency content and noise level in each signal. For the upstream velocity records and the pressure records the *power spectral density (PSD) function (autospectral density function)* was used to estimate noise levels, and for the single point records of velocity and distance taken over time above the prototype, the PSD is use to extract the oscillation frequency of each experiment. The PSD is calculated in the discrete domain as follows:

$$S_{aa} = \frac{1}{f_s N} AA^* = \frac{1}{f_s N} \mid A \mid^2 \tag{2.1}$$

Where $\mathcal{F}[a \star a] = AA^*$, $\mathcal{F}[]$ means *Fourier transform of*, $()^*$ means *complex conjugate*, f_s is the sampling frequency, and N is the number of data points.

We determined the uncertainty interval by the *Bootstrap Percentile Technique*. The bootstrap is a data base simulation method for statistical inference [8]. Based on 1000 samples for a 95% confidence interval, the MatLab function `bootstrp` was used to find the 25^{th} and the 975^{th} of the ordered statistic. The pressure measurements are reported with a 95% bootstrap confidence interval.

Fig. 2.1 presents the auto-correlation function of data examples for longitudinal velocity components (u), vertical velocity components (w), distance (d) and pressure (p). We can see that the u and w components are strongly correlated in the first second and first half second respectively; after this, both functions start decaying. For the d measurements a strong correlation is presented in the first half second, and for the p a strong correlation is presented in the first 0.01 seconds. After these times, the sampling is essentially random. In the autocorrelation for the w component (ρ_{ww}) and for the distance (ρ_{dd}) an oscillation in the function can be observed. First the autocorrelation decays and then increases before decaying again. This behavior is due to the oscillatory nature of both vertical velocity components and distance from the probe to the ribbon, since both measurements vary periodically as the ribbon oscillates.

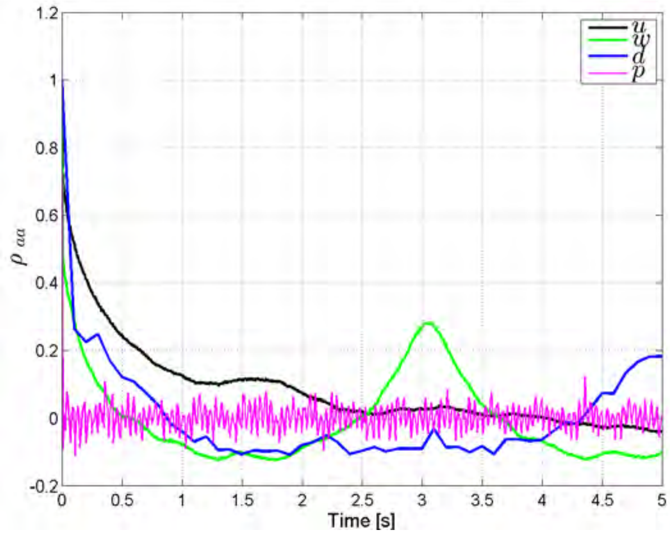

Figure 2.1: Autocorrelation functions for longitudinal velocity components (u), vertical velocity components (w), distance (d) and pressure (p).

2.3 Filtering

When required an Adaptive Gaussian filter and a Spike filter were applied to the data collected.

2.3.1 Adaptive Gaussian Filter

In order to remove the noise appearing in the data, one of the filters used was the Adaptive Gaussian Filter (Cowen and Monistmith, 1997). The filter applied is a function to threshold an adaptive Gaussian distribution to filter data that is a function of one variable assumed to be time. Based on the Student's t distribution, the algorithm filters the data to lie between a maximum and minimum value that changes dynamically based on the coefficients established. These coefficients are used to normalize the two-sided probability density function used to model the data and implemented to remove data at a given time that does not meet the threshold in any component (i.e., exceeds the bounds expected data range given the number of data points being modeled). Finally it returns the filtered data and time of such data. The filter was not applied to the matrix of the four velocity components; instead, it was implemented to each component of the velocity measurements independently, and the maximum and minimum values required by the functions came from each single component. In order to ensemble the final data matrix with the same elements removed in every direction, a triple intersection was executed (i.e., the intersection of all three components retaining only data when all three were valid).

2.3.2 Spike Filter

Due to degassing and recirculating flow, some bubbles were introduced in the flume, attaching themselves to the sensors of the ADV or affecting the sampling volume. As explained by Nori, Suzuki and Kakuno [18] it is difficult to use the ADV in bubbly flows because air bubbles generate spike noise in the ADV velocity data. The major problem is that the spike noise looks like the turbulent components in the velocity data. As a result of this, several despiking algorithms have been proposed to remove spike noise from ADV recorded velocity data [13]. Generally, Fourier low-pass filtering, moving averaging, and acceleration threshold (first differential of velocity) methods are used for removing spike noise from ADV data. The three-dimensional (3D) phase space method proposed by Goring and Nikora [13] (applied to some velocity data sets in this thesis) is an excellent method for despiking ADV data because it is efficient and does not require empirical coefficients.

2.4 Prototype description

A number of prototypes were built in order to determine the optimal configuration of the Filardo pump. Each prototype will be presented in the next chapter in the order in which the different variables were considered. The final objective of the pump is to achieve the maximum conversion of river kinetic energy to flow rate delivered at different water lifts, while maintaining a simplicity in the design, and affordability in terms of materials and construction. It must be remembered that this technology is intended for rural areas in developing countries so we want to minimize costs and increase robustness.

The first series of prototypes $T01$ explores several variables. At the beginning, different changes were made to prove that the design actually pumped water above the energy line available in the flume, essentially a proof of concept, and after the pump was proven useful, different parts were considered in the optimization. $T01$ is formed by 10 prototypes studying the influence of: separation distance between frame side bars; water depth in the flume; traversal reinforcement; internal membrane material and configuration; outlet conditions; check valve; and length and tension of strings. Then, series $T02$ explored the internal membrane material and configuration and the outlet conditions with 4 additional prototypes. A separate series called $P01$ was executed after $T02$ to understand the minor losses on the check valves in use. Eight different configurations were considered in a recirculating loop containing a pressure sensor.

The main objective of series $T03$ was to understand the effect of changing the spacing between the two plastic ribbons and the thickness of them. With 4 prototypes they also explored the internal membrane material and configuration, the way the strings were attached to the ribbon, and the outlet configuration. In the same way, series $T04$ intended to explore the effect of changing the width of the plastic ribbon. With 6 prototypes the thickness of the ribbons was also studied, as were the internal membrane materials and manufacturing process, and the outlet configuration.

CHAPTER 3

PROTOTYPES AND EXPERIMENTS

This chapter presents a detailed description of each prototype tested and a recount of the experiments related to each design. Each version is named with a unit and a decimal part, where the units change if the geometrical aspects change the whole behavior of the Prototype, and where the decimals change if within a Prototype different components are changed. In this way, for example, Prototype 2.1 is different from 2.2 since the spacing between ribbons (δ) changes without affecting the original design, and Prototype 2.1 is different from Prototype 3.3 since the width of the plastic sheets are different with consequences in the oscillation patterns and force induced in the internal membrane. In the same way, the tests related to each prototype are identified with a T (P for the minor loss coefficient test) followed by a two unit number. Prototype 1 is related to test series $T01$ and $T02$, the minor loss coefficient prototype to $P01$ to $P08$, Prototype 2 to test series $T03$, and finally Prototype 3 is tested under $T04$ series.

For clarity, the analysis of the data will be presented in the following chapter.

3.1 Prototype 1.1 Series $T01$

This section presents the changes introduced within Prototype 1.1 in order to prove that the concept effectively lifts water above the energy grade line. The changes that will be explained in detail are the selection and design of an internal membrane, the spacing between ribbons, supporting steel bars, tension in the strings, check valve, outlet design and transversal reinforcement.

3.1.1 Description

The ribbons are polypropylene copolymer (Plastics International, MN, USA), with physical and mechanical properties presented in Table 3.1. Each ribbon is 0.60*m* (23.6*in*) long, 0.30*m* (12.0*in*) wide, with a thickness of 0.50*mm* (0.02*in*) for test series $T01$.

The membrane is constructed from a tubular type material, a multilayer plastic film (Diaper Genie Disposal System, Playtex Products, LLC), 0.60*m* long, 0.25*m* wide, open on both sides, that can be easily manipulated to build a sealed chamber, adding negligible rigidity to the mechanism.

The side bars are 2" aluminum 90^o angles, 0.91*m* long, with a wall thickness of 0.32*cm* (1/8*in*). A threaded rod, 0.79*cm* (5/16*in*) diameter sets the separation between side bars (Fig. 3.1).

Microfilament braided line, 0.43*mm* diameter, made of Spectra fiber (80 *punds* Power Pro, Shimano American Corporation), is used for the strings. Separation between strings on the ribbon is 2.9*cm* (1.15*in*), while on the side bars is 2.45*cm* (0.965*in*). The strings are tied to the edge of each ribbon, and pass through a 1*mm* diameter hole in the side bars. Wire-lockable 18-8 stainless steel socket head screws (McMaster-Carr, OH, USA) are used to adjust the string length from the ribbon edges to the side bars (Fig. 3.1).

The ribbon is mounted on a frame made of extruded aluminum alloy (McMaster-Carr, OH, USA). The frame rests on the top of the flume and four legs extend into the water, allowing the ribbon pump to be set at different locations along the flume and at different elevations within the water column (Fig. 3.1 *right*).

Table 3.1: Properties of polypropylene ribbons as provided by manufacturer (Plastics International).

Property	Value	Units	Test method
Density	55.08	lbs/ft^3	ASTM D-792
Water absorption	0.01	%	ASTM D-570
Yield point	3466	psi	ASTM D-638
Elongation at yield	11	%	ASTM D-638
Tensile break	4814	psi	ASTM D-638
Elongation at break	649	%	ASTM D-638
Tensile modulus	152192	psi	ASTM D-638
Flexural modulus	183860	psi	ASTM D-790
Flexural strength	3741	psi	ASTM D-790
Izod impact	7.8	$ft \cdot lb/in$	ASTM D-4020
Tensile impact	384	$ft \cdot lbs/in^2$	DIN 53448
Hardness	73	$Shore\, durometer$	ASTM D-2240

In some of the tests (Table 3.2), the polypropylene sheets were reinforced transversally with 4 stainless steel (SS) strips, 0.46*mm* by 25.4*mm*, and with 10 wood dowels (WD) (5/16*in* diameter).

3.1.2 Experiments

The first series of experiments, referred to as $T01$, used 0.50*mm* (0.02*in*) thick ribbons. For all $T01$ tests, the mean position of the ribbon was located 15.2*cm* (6*in*) above the bottom of the flume. The mechanism was tested for two separation distances between side bars: 0.45*m* and 0.36*m*, with each string individually ad-

Figure 3.1: Ribbon pump, series $T01$. Top view (*left*) and side view mounted on the frame suspended on top of the flume (*right*).

justed for each case, to obtain the initial tension required to deform the ribbons into a single period sinusoid. A summary of the experiments is presented in Table 3.2.

The $0.50mm$ thick ribbons can not withstand by themselves the pressure buildup inside the membrane as the water is pumped through.. As seen in Fig. 3.2 (*left*), the plates deform laterally, forming a “pipe” which stops the expected oscillations. The polypropylene sheets were reinforced transversally with 4 stainless steel (SS) strips, $0.46mm$ by $25.4mm$, (Fig. 3.2 *right*) and with 10 wooden dowels (WD) ($6.4mm$ diameter) for subsequent tests, minimizing the lateral deformation effect shown in Fig. 3.2. However, for all cases, when the outlet is constrained, either by a contraction, or any fittings required to introduce the exit pipe, the pressure builds up inside the membrane perturbing or even arresting the ribbon’s oscillations. We will refer to the outlet conditions as “free” when the tubular membrane is fully open, and “constrained” when the outlet pipe is in place. The shortest separation distance W_r tested (Tests $T01B$) showed more consistent oscillations, since for the tests $T01A$ ribbon motions often died out and required restarting by hand. In addition, for tests $T01A03$ and $T01B01$ the fully-open membrane extended downstream of the ribbon by $10cm$

Table 3.2: Parameters for experiments series $T01$, separation between side bars W_r, water depth H, type of reinforcement, outlet conditions and resulting motions.

Test	W_r (m)	H (m)	transversal Reinforcement	Outlet Conditions	Successful oscillations?
$T01A01$	0.450	0.300	None	Constrained	No
$T01A02$	0.450	0.300	4 SS	Constrained	No
$T01A03$	0.450	0.325	4 SS	Free-Longer extending downstream	No
$T01A04$ t1	0.450	0.325	4 SS	Free	Yes
$T01B01$ t2	0.360	0.370	4 SS	Free-Longer extending downstream	Yes
$T01B02$t3	0.360	0.370	4 SS	Free	Yes
$T01B03$t4	0.360	0.370	4 SS, 10 WD	Constrained	Yes
$T01B04$t5	0.360	0.370	4 SS, 10 WD	Constrained	Yes
$T01B05$t6	0.360	0.370	4 SS, 10 WD	Constrained	Yes
$T01B06$t7	0.360	0.370	4 SS, 10 WD	Free	Yes

to test for the effects of transitions downstream. The extra-long membrane completely suppressed ribbon motions in $T01A03$, but allowed the oscillations in the configuration for $T01B01$. It is assumed that the extending membrane acts in a similar way as the splitter plate behind a cylinder, suppressing vortex shedding and breaking up the vortices that contribute to the ribbon motions. Analysis of the velocity field on a vertical plane using particle image velocimetry (PIV) will provide better information as to the effects of the outlet configuration.

For this specific set of experiments the flow speeds studied were between $0.35m/s$ and $0.80m/s$, set by running both recirculating pumps at frequencies from $20Hz$ to $40Hz$. Each test is identified hereafter by the pump frequency (e.g., $Q20$,$Q40$). Analysis focuses on subseries $T01B$ ($36cm$ separation), since it proved

Figure 3.2: Deformed non-reinforced ribbon (*left*), and reinforced with thin stainless steel strips (*right*).

more consistent than the subseries $T01A$.

From the distance-check ADV records, we get the actual displacement of the ribbon, as shown in Fig. 3.3 (*left*), where the distance from the probe head to the ribbon surface d (m) is plotted for all flow speeds. It is clear that the frequency of the motions increases with the flow speed, while the amplitude, which is set mainly by the strings length, remains almost constant.

Frequencies and amplitudes are calculated from the distance and velocity records. It is apparent in Fig. 3.3 (*right*) that the frequencies of the ribbon oscillations and those of the passing vortices match for all flow speeds, as identified in the frequency spectra for velocity and distance records.

The frequencies and amplitudes obtained from all $T01B$ experiments are shown as a function of flow speed U measured upstream of the ribbon pump in Fig. 3.4. The frequency of ribbon motions increases with velocity in all cases, but there is no single relationship between experiments, indicating that small variations in the configuration of the prototype can lead to different behaviors. The amplitude of the motions, ideally set by the length of the strings, also changes between tests but does not show a clear trend as a function of flow speed.

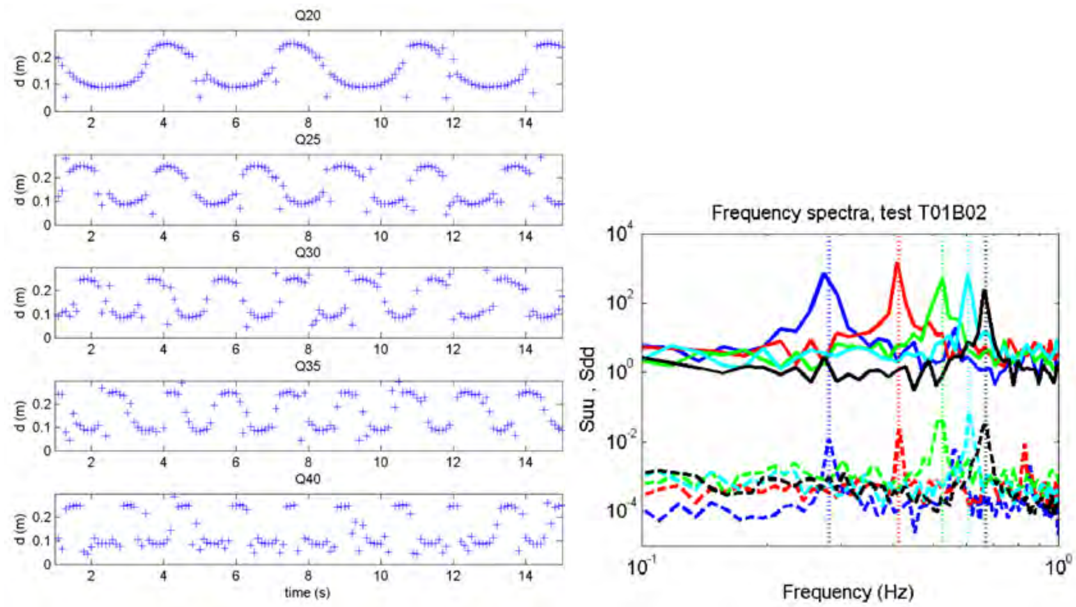

Figure 3.3: Displacement measured for test $T01B01$ at increasing flow speeds (*left*). Frequency spectra for flow rates $Q20$ through $Q40$, test $T01B02$, obtained from velocity records - dashed lines - and distance records - solid line - (*right*).

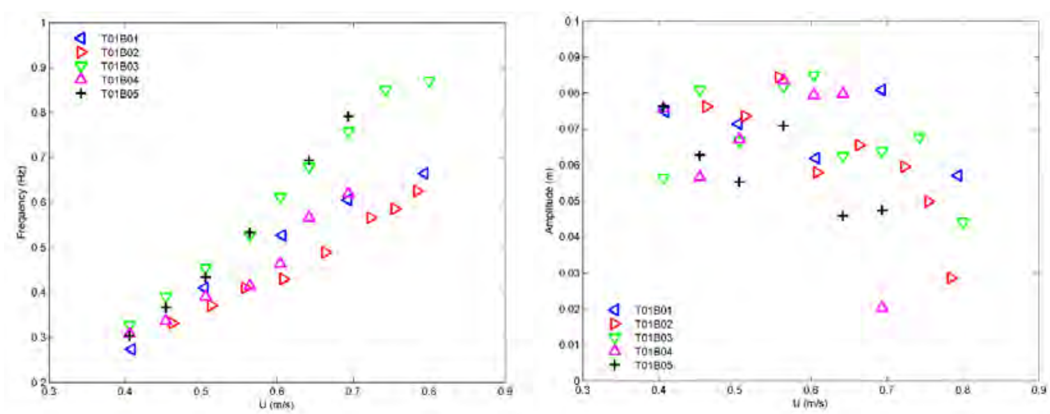

Figure 3.4: Frequency of the ribbon oscillations as a function of flow speed for all $T01B$ tests (*left*). Amplitudes of the ribbon oscillations as a function of flow speed for all $T01B$ tests (*right*).

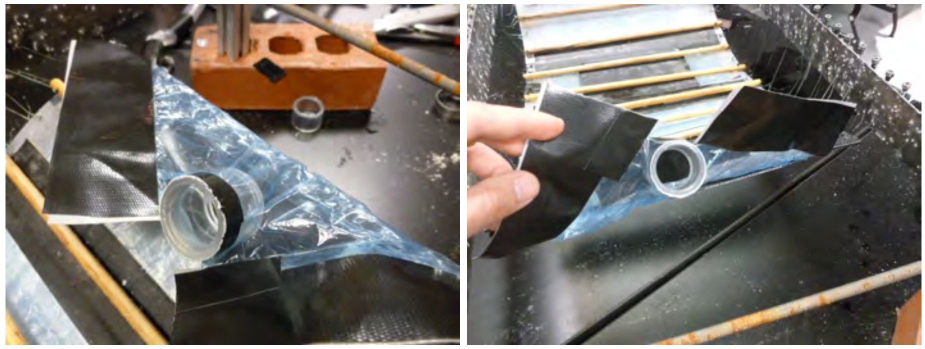

Figure 3.5: Outlet configuration for Prototype 1.1 for test $T01B06$.

It is evident from Fig. 3.4 that the frequency increased when the wooden dowels were added to the ribbons, giving more transversal rigidity to the prototype and almost eliminating the bulging effect. Tests $T01B03$, $T01B04$, and $T01B05$ varied only in the setting of the outlet pipe. The lower frequencies observed in $T01B04$ are assumed due to the outlet being fixed to the downstream threaded rod, which partially restrained the free movement of the downstream ribbon edge.

For the final configuration of Prototype 1.1 ($T01B06$ with an unrestricted outlet), 2.5*cm* of a 3/4*in* ID translucent plastic pipe was held with heavy duty duct tape (Gorilla Tape®) to the customized outlet of the internal plastic membrane (Fig. 3.5). To this first pipe, a clear PVC Schedule 40 coupling of 3/4*in* nominal diameter was added with another 15*cm* of a 3/4*in* ID translucent plastic pipe. To this last pipe, a finger of a latex glove was added to provide flexibility in this configuration. After another 30*cm* of the plastic pipe, a one way valve for a CPR responder masks (Allied 100, LLC) was attached to prevent back-flow. After this valve, 5*cm* of plastic pipe, a 3/4*in* coupling and 1.5 meters of the same translucent pipe were attached to complete the outlet.

3.2 Prototype 1.2 Series $T02$

This section presents the changes and tests for Prototype 1.2. The modifications to the internal membrane, the outlet and the final definition of the separation between steel bars leads to better performance in this version.

3.2.1 Description

This prototype differs from the previous one in the tubular membrane, the configuration of the outlet and the separation between side bars.

The tubular membrane is a VetOne OB Sleeve by Ag-Tek®, 36*in* long and 0.11*mm* thick, made of 100% Polyethylene, open on one side, providing an already built sealed chamber and with a narrow exit as well as adding negligible rigidity to the mechanism.

The outlet (Fig. 3.6) is composed of a series of flexible pipes, PVC couplings, a flexible membrane and a CPR valve. First, 5*cm* of a 3/4*in* ID translucent plastic pipe was held with heavy duty duct tape to the middle finger of the veterinary plastic glove described above. To this first pipe, a clear PVC Schedule 40 coupling of 3/4*in* nominal diameter was added, preserving the onfiguration of the outlet from Prototype 1.1.

The separation between side bars was held constant at 0.36*m*, with each string individually adjusted for each case, to obtain the initial tension required to bend the ribbons into a single period sinusoidal deformation.

For all tests (Table 3.3), the polypropylene sheets were reinforced transver-

Figure 3.6: Outlet configuration for the Prototype 1.2.

sally with 4 stainless steel (SS) strips, 0.46*mm* by 25.4*mm*, and with 10 wood dowels (WD) (5/16*in* diameter).

3.2.2 Experiments

The second series of experiments, referred to as $T02$, used 0.50*mm* (0.02*in*) thick ribbons. For all $T02$ tests, the mean position of the ribbon was located 15.2*cm* (6*in*) above the bottom of the flume. The mechanism was tested for only one separation between side bars (0.36*m*), with each string individually adjusted to obtain the initial tension required to deform the ribbons. A summary of the experiments is presented in Table 3.3.

As described previously the tubular membrane is VetOne OB Sleeve. The use of heavy duty duct tape to create the outlet for the multilayer plastic film demonstrated a constant decay of performance during the $T01$ experiments. The use of the sleeve prevented the decay in performance for $T02$ experiments.

For tests $T02A01$ successful oscillations were obtained, but the rigidity of the outlet pipe reduced the regularity of such movements, therefore reducing sig-

Table 3.3: Parameters for experiments series $T02$, separation between side bars W_r, water depth H, type of reinforcement, outlet conditions and resulting motions.

Test	W_r (m)	H (m)	transversal Reinforcement	Outlet Conditions	Successful oscillations?
$T02A01$	0.360	0.370	4 SS, 10 WD	Free, complete plastic pipe plus CPR valve	Yes
$T02A02$	0.360	0.370	4 SS, 10 WD	Free, complete plastic pipe plus metallic check valve	Yes
$T02A03$	0.360	0.370	4 SS, 10 WD	Constrained, complete plastic pipe plus metallic check valve	Yes
$T02A04$	0.360	0.370	4 SS, 10 WD	Free, plastic pipe, flexible membrane and CPR valve	Yes

nificantly the outflow. For test $T02A02$ the CPR valve was replaced with a $3/4in$ NPT Threaded Swing Check Valve resulting in a better performance of the seal created by the metallic valve. For this test, first, there was no outflow, meaning the flow inside the valve was not sufficient to let the valve perform as expected, and second, the rigidity of the outlet pipe still affected the regularity of the oscillations. Test $T02A03$ was an attempt to improve the performance of the metallic valve, which in this case was placed to force the flow vertically through it. This case was not successful in trying to use both the gravity force and the back-flow action to improve a seal of the check valve. The final configuration was obtained in $T02A04$. A flexible membrane was introduced to improve the regular movement of the ribbon, and with the use of the CPR valve the results presented in Chapter 4.2 were obtained.

3.3 Minor losses on check valve

This section contains the study of the check valve intended to prevent back flow. Different tests were conducted to measure the drop in pressure as water flows through the selected valve. A detailed description of the check valve, the experimental set-up, and the results are included here-in.

3.3.1 Description

The basic concept of the prototype is to transports water by creating a pinch point or constriction which travels from the entrance to the end of the ribbons, and by those means the pump moves water from one end to the other; analogously with a peristaltic pump. After the polypropylene sheets, the outlet pipe contains a check valve to prevent back-flow. A minor loss is introduced with this check valve and its effects must be evaluated in order to improve the performance of the current or future prototypes. The valves tested are first, a simple air check valve used in fish tanks (Fig. 3.7), and second, a CPR responder masks from Allied 100, LLC (Fig. 3.8). It is expected that by introducing the series of expansion and contractions from both the valves and the fittings, zones of flow separation will occur [27], and as a consequence large head losses will be present in the prototype. It is well understood that by improving the efficiency of the valve in use (i.e., better water seal and minor geometry changes) the performance of the prototype can be enhanced. From the valve in Fig. 3.7 poor performance is expected. The plastic cone inside this valve provides a reasonable seal for back-flow, however it is too rigid and does not move with ease to provide enough room for the water to flow freely. On the other hand, the valve

Figure 3.7: Check Valve for fish tanks

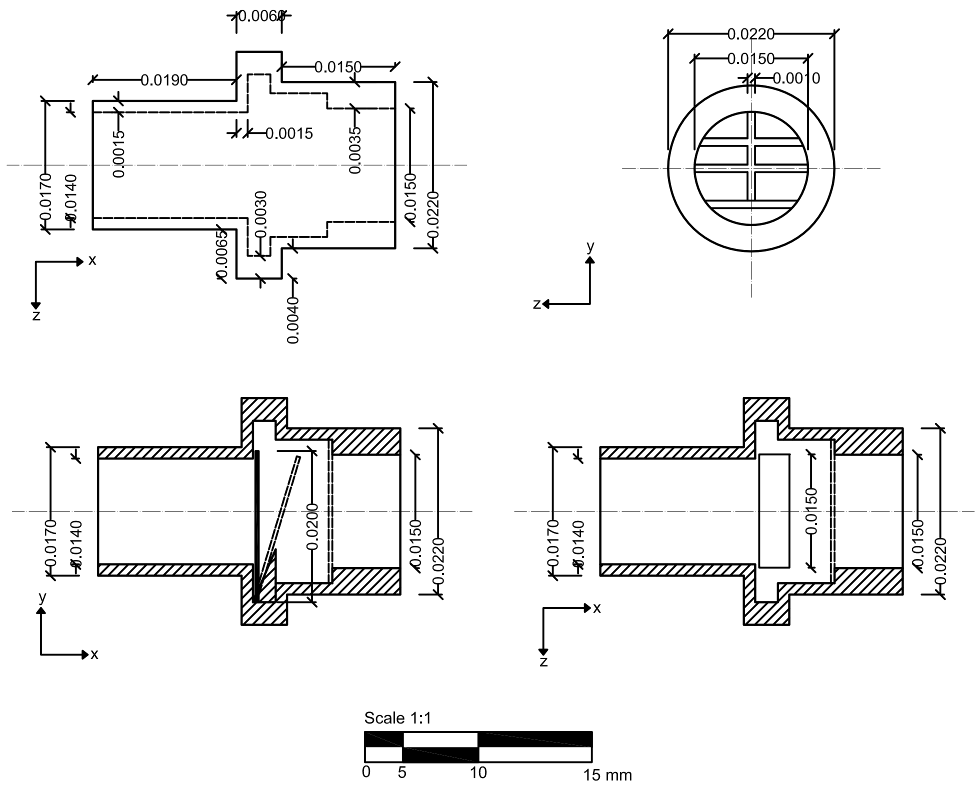

Figure 3.8: Check Valve: CPR valve for responder masks (Allied 100, LLC).

in Fig. 3.8 provides a better seal by means of a flexible plastic membrane, but still the geometry will introduce important head losses.

3.3.2 Experiments

Two different experiments were conducted to determine the best valve for the early prototypes. The seepage rate was measured as a metric of the back flow seal performance, while the minor loss coefficient was measured to establish the energy loss introduced by the valve with the best water seal.

3.3.2.1 Seepage rate

In order to determine the seepage rate the two valves where placed in a vertical position (i.e., the flow direction of the valves was pointing upwards) at the end of plastic pipes held in a vertical straight line. The pipe lines contained water under pressure which was applied against the water seal. A vacuum was produced to hold in place the water which was then released to start the experiment at $t = 0sec$. A $^1/_4in$ OD, $0.170in$ ID polyethylene pipe (Freelin Wade Co.) was used for the valve presented in Fig. 3.7, and a $1.0in$ OD, $^3/_4in$ ID clear vinyl tubing (Watts Co) was used for the second valve presented in Fig. 3.8.

The water head reported in Fig. 3.9 was measured form the seal provided by the valves to the water-air interface present in the water column. As can be seen from the figure on the left, the fish tank valve is very inefficient as a check valve. The water column rapidly descends from $h = 131cm$ at $t = 0min$ to $h = 26cm$ at $t = 8.2min$, and to $h = 4.5cm$ at $t = 39.6min$. On the other hand, the CPR valve presented on Fig. 3.8 demostrates a better performance according to Fig. 3.9 on the left. The water column reflects an almost linear descent through time going from $h = 161cm$ at $t = 0min$ to $h = 91.4cm$ at $t = 95.0min$, point where the behavior starts to flatten out. For this valve, after $t = 443.9min$, h remained at a level of $15.7cm$. The same behavior can be drawn from the second figure at the left. The fish tank valve starts with $q = 0.4L/h$ at $t = 0min$ and $h = 131cm$, and rapidly descends to $q = 0.03L/h$ at $h = 26cm$ and $t = 8.2min$. By the end of the experiment, only $2.4cm$ of water head remained in the pipe, which suggested the water seal was not efficient. On the other hand, the CPR valve started with a seepage rate of $q = 0.17L/h$ at $t = 0min$ and $h = 161cm$, and descended in an almost straight line to $q = 0.05L/h$ at $t = 208.4min$ and $h = 44.8cm$. By the end of the experiment, with $t = 443.9min$ and $q = 0.01L/h$ the remaining water head on the pipe was $h = 15.7cm$.

Based on this results, the CPR valve is implemented in the prototypes presented in this document. The time scale of the experiments that determine the flow rate of the pump is at most $10min$, only 2.2% of the time scale of the experiment conducted on the CPR valve. In the same way, the maximum water head to overcome will be $25cm$ (the maximum height the outlet pipe was lifted measured from the still water level to the lower inner edge of the pipe in the flow rate experiments), which represents a 6.4% of the maximum water head in the seepage experiments. Finally, if the water head to overcome is $25cm$, the seepage rate expected is around $q = 0.025L/h$ which is three orders of magnitude less than the flow rate expected for the pump.

3.3.2.2 Loss coefficient of CPR valve

Apart from the seepage rate expected for the valve in use, the minor loss coefficient was required to fully describe the performance of the check valve. As can be seen from Fig. 3.8, the left end of the valve does not fit exactly into a $3/4in$ PVC coupling (attached to the end of the prototype), requiring a sudden contraction

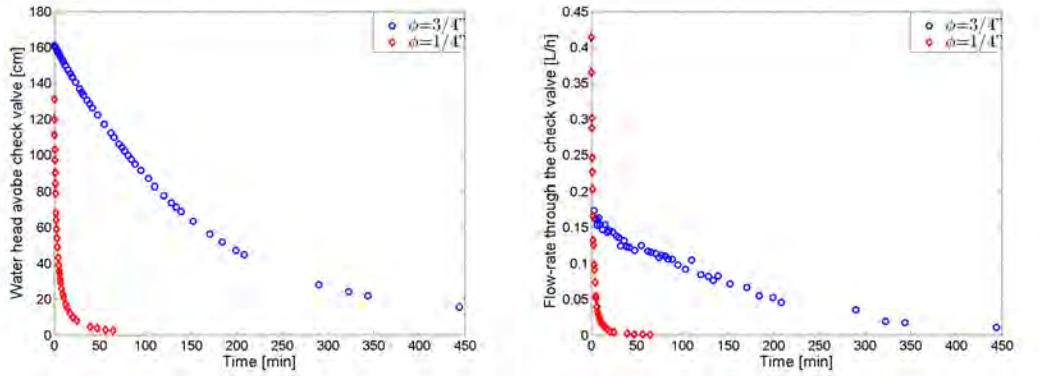

Figure 3.9: Seepage rate for the check valves: water head (*left*) and flow-rate (*right*).

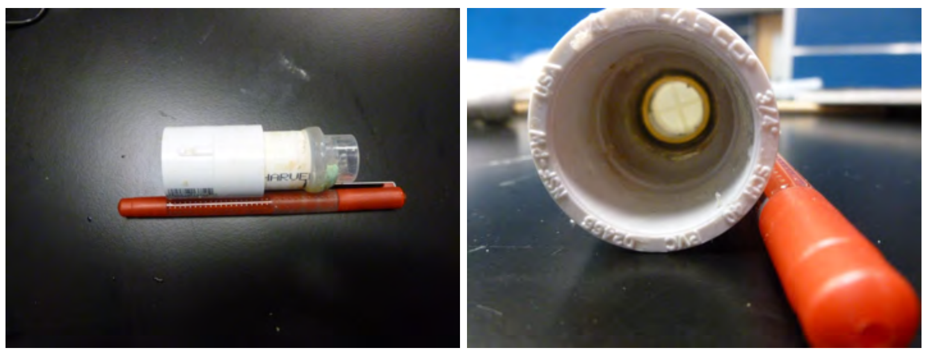

Figure 3.10: PVC fittings machined for the CPR valve. General view including the $3/4in$ PVC coupling fitting from the prototype (*left*) and internal PVC ring (gray) included as a connection between the $17mm$ end of the CPR and the $3/4in$ ND PVC pipe attached (*right*).

in order to create a water seal. A Schedule 40 $3/4in$ PVC pipe was attached to the valve (Fig. 3.10 *left*) and a machined PVC ring (Fig. 3.10 *right*) was introduced between the valve and the $3/4in$ PVC pipe in order to fill the gap ($\sim 3.4mm$). This contraction and the additional geometry changes presented in Fig. 3.8 introduce zones of flow separation and as consequence head loss.

The general set-up shown in Fig. 3.11 presents the configuration of the minor loss coefficient experiments. The water flow is driven by a small pump (submersible pump Model 5-MSP, 115V-60H, 5.0 AMP, by Little Giant®). For tests $P01$ and $P02$ (Table 3.4) this pump was connected before the valve controlling the water flow entering the system. Since it was detected that noise coming from the pump was affecting the data measurements, a water reservoir was introduce to reduce it. For experiments from $P03$ to $P08$ the pump was connected to the reservoir, and the water entering the system always had a constant head of $47cm$ controlled by a needle valve and the overflow orifice in the tank. The low flow rates entering the system where controlled by the micro threads of the needle valve, which provided visual reference points to repeat settings on a color coded scale. After the valve, a $^1/_4in$ OD, $0.170in$ ID polyethylene pipe (Freelin Wade Co.) entered the system with a PVC cap connection, then, the water traveled through $40cm$ of Schedule 40 $^3/_4in$ PVC pipe until it encounters the check valve attached to the end of this pipe, and then another $55cm$ through a $1.0in$ OD, $^3/_4in$ ID clear vinyl tubing (Watts Co) to the exit.

The pressure gauges were connected to the system through two pieces of $25cm$ of a $^1/_4in$ OD, $0.170in$ ID polyethylene pipe (Freelin Wade Co.). To provide a differential pressure measurement, one end of the pipe was connected to the pressure gauge and the other end to a hole either $20cm$ upstream or downstream the check valve. Two different pressure gauges were used: $7KPa$ and $2inH_2O$. The first one, OMEGA's PX26-001DV series pressure sensor is a PC mountable wet/wet differential pressure sensor with a maximum voltage of $16.7mV$ and a corresponding value of $7KPa$. The second one, is a low range wet/wet differential pressure transducer by Omegadyne Inc with a maximum voltage of $5V$ and a corresponding value of $2inH_2O$. Each data point is reported based on a record length of 10,000 samples at $100Hz$.

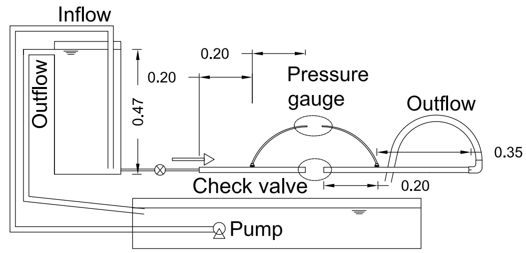

Figure 3.11: General configuration for the minor loss coefficient experiment.

Table 3.4 shows the experiments carried out under the configuration presented on Fig. 3.11. As described above, *P*01 was not successful due to the noise coming from the pump driving the flow. The fact that the pump was connected directly to the pipes did not provide a constant flow rate, introduced noise from its operation and prevented accurate control when a low flow rate was required. This experiment also experience problems with the connection to the data aquisition server. Data aquisition was done online, which meant the information traveled from the sensor to the primary server and back to the acquisition computer through the wires and connections in the DeFrees Hydraulic Laboratory and Hollister Hall. In this path, the signal picked up noise from different processes [9] occurring in the facilities and could be attributed to thermal noise, presence of high voltage lines, operation of pumps, among others. Test *P*02 was an attempt to reproduce the same first configuration and dismiss possible human errors introducing noise. Since the result was the same, *P*03 was intended to remove the noise coming from the pump by introducing the water reservoir shown in Figure 3.11. This tank helped to eliminate the noise from the incoming flow rate and provided a constant water head and a better way to control the volume of water entering the system.

Despite the elimination of the noise from the removal of the pump, the online data aquisition connection to the server was still introducing a considerable amount of noise. For $P03$ the standard deviation (σ) was of the same order as the mean of the pressure drop through the system ($\overline{\triangle P}$), and as consequence $P04$ intended to suppress the noise from the server connection. A stand along data acquisition computer was employed and showed a considerable improvement. The maximum standard deviation was around 10% of the pressure drop ($\sigma \sim 0.1\overline{\triangle P}$). Taking this configuration into consideration, $P05$ was conceived to gather more data points on the lower flow rates (i.e, from $1L/h$ to $30L/h$), but a water leakage prevented it from being successful.

Table 3.5 shows the results for the last experiment ($P06$) run with the $7KPa$ pressure gauge. This experiment contained 9 data points between what it is considered the operational rage of the pump ($0L/h$ to $30L/h$). The standard deviation was consistent throughout the test and the behavior of the minor loss coefficient defined as Eq. 3.1 from Munson, Young and Okiishi [19] ($\rho = density$ and $u = velocity$), and shown in Fig. 3.12 (*left*) appeared to be stable, but despite this consistency, results of K_m on the order of $thousands$ were considered extreme and so the accuracy of the $7KPa$ pressure gauge was questioned.

$$K_m = {}^{\triangle P}/_{0.5\rho u} \tag{3.1}$$

The data acquired in $P07$ strived for precision and accuracy with the $2inH_2O$ pressure transducer. As shown in Table 3.6 both values of $\triangle P$ and K_m were reduced. The Table reports also the maximum and minimum values along with the 95% bootstrap confidence interval [8]. From Fig. 3.12 (*right*) we can conclude that for the operational rages of the pump the minimum K_m expected is 6.2 for $Q = 30L/h$ and $R_e = 756$. The general behavior of K_m starts with a negative slope

Table 3.4: Parameters for experiments on CPR valve

Test	Pressure gauge	Server Conditions	Successful?	Description
$P01$	$7KPa$	On-line server	No: noise affecting the data acquisition	Acquisition system connected to the online server and pump driving the flow attached to the pipes.
$P02$	$7KPa$	On-line server	No: noise affecting the data acquisition	Acquisition system connected to the online server and pump driving the flow attached to the pipes.
$P03$	$7KPa$	On-line server	No: noise affecting the data acquisition	Acquisition system connected to the online server and pump driving the flow attached to a reservoir to suppress noise from the pump.
$P04$	$7KPa$	Stand alone server	Yes: noise was reduce (σ of $\triangle P$ less than 10% of it)	Acquisition system connected to the stand alone server and pump driving the flow attached to a reservoir.
$P05$	$7KPa$	Stand alone server	No: water leak was detected on the system	Acquisition system connected to the stand alone server and pump driving the flow attached to a reservoir.
$P06$	$7KPa$	Stand alone server	Yes: noise was present at lower flow rates	Acquisition system connected to the stand alone server and pump driving the flow attached to a reservoir.
$P07$	$2inH_2O$	Stand alone server	Yes: new pressure gauge increased the precision on $\triangle P$ value	Acquisition system connected to the stand alone server and pump driving the flow attached to a reservoir.
$P08$	$2inH_2O$	Stand alone server	Yes: new pressure gauge increased the precision on $\triangle P$ value	Acquisition system connected to the stand alone server and pump driving the flow attached to a reservoir.

Table 3.5: Statistics of $P06$

$Q[L/h]$	Re	$\triangle P[Pa]$	$\sigma[Pa]$	Km
2.1	52	33.79	5.66	4891
3.0	76	34.77	5.64	2377
4.7	119	36.60	5.73	1006
6.9	173	39.02	5.69	507
9.1	230	41.55	5.71	308
10.9	275	43.47	5.74	225
13.7	344	47.33	5.71	156
17.0	428	51.85	5.71	111
25.4	641	66.29	5.65	63
37.7	951	115.73	5.86	50
45.6	1151	146.59	6.14	43
52.8	1330	177.90	6.50	39
108.0	2723	514.46	6.50	27
144.0	3631	922.93	16.62	27
359.2	9056	4067.59	73.05	19

until it reaches a horizontal line at a point where the transition from laminar to turbulent flow starts in the experimental set up ($R_e = 885$). Then, the minor loss coefficient presents a positive slope, reaches a horizontal line, and finally starts to descend with a negative slope in the turbulent regime.

Test $P08$ was performed to confirm the repeatability of the data in the previous test and the results are presented in Table 3.7 and Fig. 3.13 (*left*). The first thing to highlight are the three points that appear to be biased in error low ($Q = 16.3L/h$, $Q = 18.8L/h$ and $Q = 22.5L/h$), located near the expected transi-

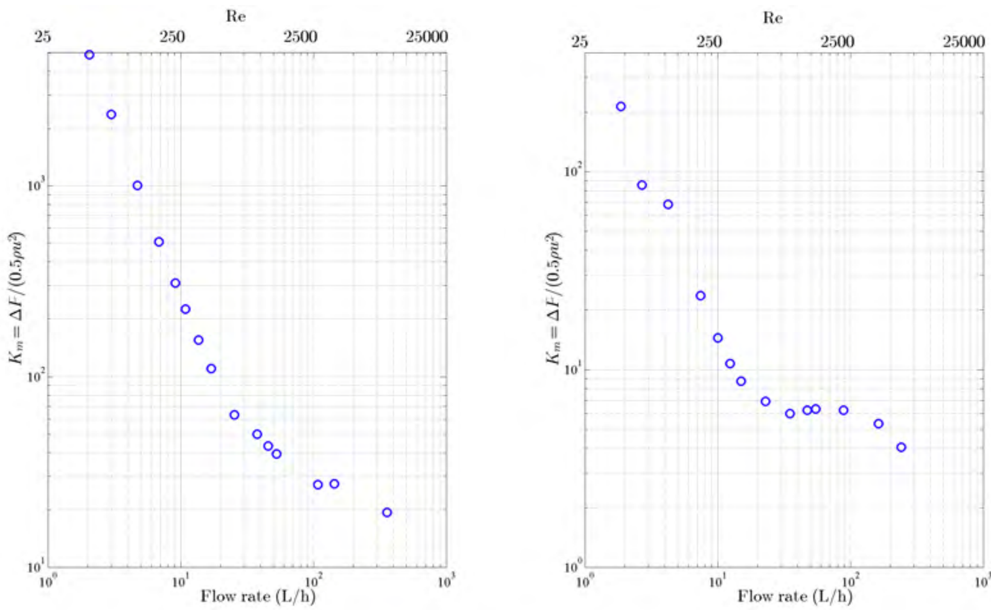

Figure 3.12: Check valve minor loss coefficient as function of flow rate (*Re*) for test *P*06 (*left*) and test *P*07 (*right*).

tion point. Beyond this discrepancy, the general behavior of *P*08 resembles the results from *P*07 as can be seen in Fig. 3.13 (*right*).

3.4 Prototype 2 Series *T*03

This section details the changes made in the prototype to understand the influence of changing the thickness of the ribbons, the material and design of the internal membrane, the material of the transversal reinforcement, the spacing between ribbons, and the outlet design.

Table 3.6: Statistics of $P07$

$Q[L/h]$	Re	$\triangle P[Pa]$	$\sigma[Pa]$	$Max[Pa]$	$Min[Pa]$	95% $Confidence\ Interval$ $[Pa]$		Km
1.9	47	−1.21	0.28	−0.33	−2.03	−1.197	−1.221	214.6
2.7	68	−1.00	0.30	0.01	−1.93	−0.991	−1.011	85.5
4.2	107	−1.99	0.29	−0.72	−3.10	−1.968	−2.008	68.2
7.4	187	−2.11	0.28	−1.11	−3.15	−2.090	−2.132	23.5
10.1	253	−2.39	0.29	−0.91	−3.54	−2.361	−2.409	14.5
12.4	313	−2.69	0.27	−1.93	−3.49	−2.663	−2.717	10.8
15.0	378	−3.19	0.29	−2.32	−4.02	−3.162	−3.227	8.7
22.9	577	−5.90	0.27	−5.04	−6.74	−5.840	−5.958	6.9
35.1	885	−12.02	0.35	−10.68	−13.06	−11.904	−12.146	6.0
47.4	1194	−22.77	0.61	−20.64	−25.54	−22.543	−23.001	6.2
54.8	1382	−30.89	0.75	−28.31	−34.04	−30.581	−31.202	6.3
88.7	2236	−79.62	1.75	−72.76	−86.51	−78.824	−80.425	6.2
162.8	4104	−230.15	3.92	−215.49	−242.45	−227.836	−232.463	5.3
241.0	6075	−382.05	5.80	−352.92	−409.85	−378.211	−385.891	4.0

3.4.1 Description

The Prototype 2 ribbons are made of polypropylene copolymer (Plastics International, MN, USA), with physical and mechanical properties presented in Table 3.1. Each ribbon is 0.60*m* (23.6*in*) long, 0.30*m* (12.0*in*) wide, with a thickness of 0.80*mm* (0.03*in*) for test series $T03$, (0.01*in* more than Prototype 1.1 and 1.2). For series $T03$, 1/8*in* ID copper grommets by METALgrommets.com where pierced through the wholes where each string is tied to the ribbon, preventing the tension on the strings and its constant oscillation from tearing the polypropylene; a problem in previous prototypes. Fig. 3.14 shows the implementation of the

Table 3.7: Statistics of $P08$

$Q[L/h]$	Re	$\triangle P[Pa]$	$\sigma[Pa]$	$Max[Pa]$	$Min[Pa]$	$5\%\ Confidence\ Interval\ [Pa]$		Km
1.4	36	−1.22	0.11	−0.79	−1.67	−1.203	−1.227	375.6
2.0	49	−1.28	0.11	−0.84	−1.67	−1.270	−1.295	205.3
3.0	75	−1.48	0.11	−1.04	−1.91	−1.465	−1.495	103.1
4.4	110	−1.67	0.11	−1.23	−2.06	−1.658	−1.691	54.4
6.5	163	−2.10	0.11	−1.67	−2.49	−2.074	−2.116	30.7
9.0	228	−3.00	0.12	−2.54	−3.42	−2.966	−3.027	22.6
12.3	310	−4.69	0.14	−4.19	−5.17	−4.645	−4.740	19.1
16.3	410	2.02	0.16	2.65	1.44	2.002	2.042	4.7
18.8	473	1.24	0.18	1.93	0.47	1.232	1.257	2.2
22.5	568	−0.68	0.31	0.61	−1.86	−0.677	−0.691	0.8
33.1	833	−7.22	0.23	−6.38	−8.08	−7.145	−7.290	4.1
47.0	1185	−21.95	0.80	−18.72	−25.08	−21.728	−22.169	6.1
68.4	1725	−46.94	1.61	−40.58	−53.11	−46.467	−47.411	6.2
80.8	2038	−68.06	3.44	−58.51	−81.39	−67.379	−68.748	6.4
117.2	2956	−149.61	3.20	−137.50	−161.54	−148.110	−151.118	6.7
140.4	3540	−200.17	3.55	−186.08	−214.79	−198.160	−202.184	6.2
160.4	4044	−245.40	3.51	−231.64	−258.90	−242.932	−247.865	5.9
219.6	5537	−339.17	8.95	−301.06	−370.97	−335.755	−342.573	4.3
249.9	6301	−443.95	8.13	−411.73	−469.68	−439.483	−448.408	4.4

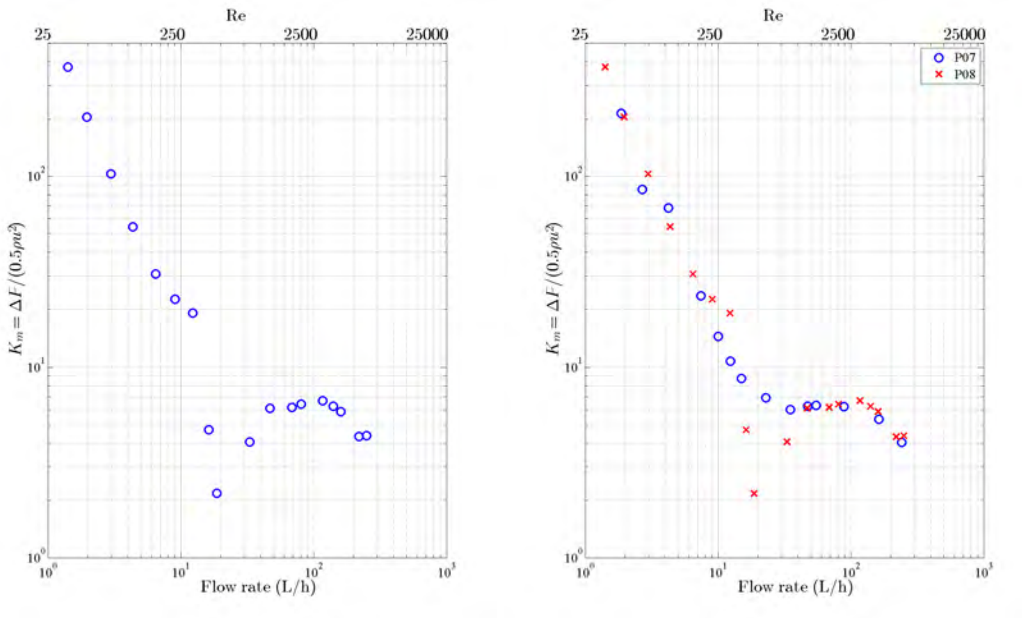

Figure 3.13: Check valve minor loss coefficient as function of flow rate (*Re*) for test *P*08 (*left*) and test *P*07 with test *P*08 (*right*).

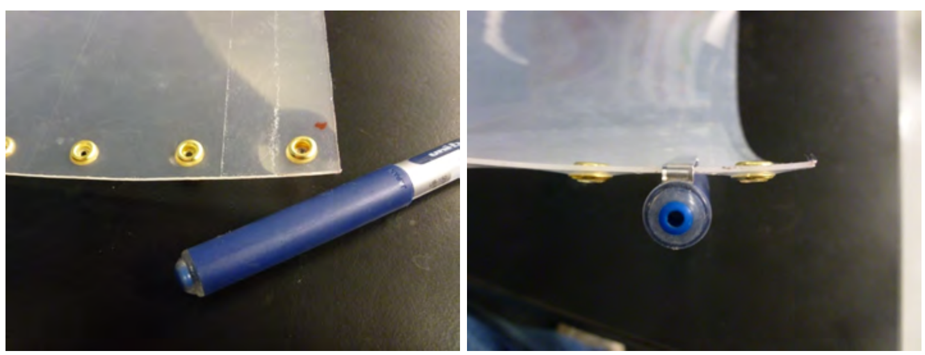

Figure 3.14: Grommets implemented in Prototype 2 Series *T*03: these copper grommets prevented the rupture of the polypropylene sheets under the constant tension and oscillations coming from the strings attaching the prototype to the metalic frame.

grommets in the first holes.

The tubular membrane for Series *T*03 is a polyethylene sheet 0.005*in* (0.127*mm*) thick. As can be seen in Fig. 3.15 left, the plastic was heated to create the water proof seal. All the tubular membranes used in these series of

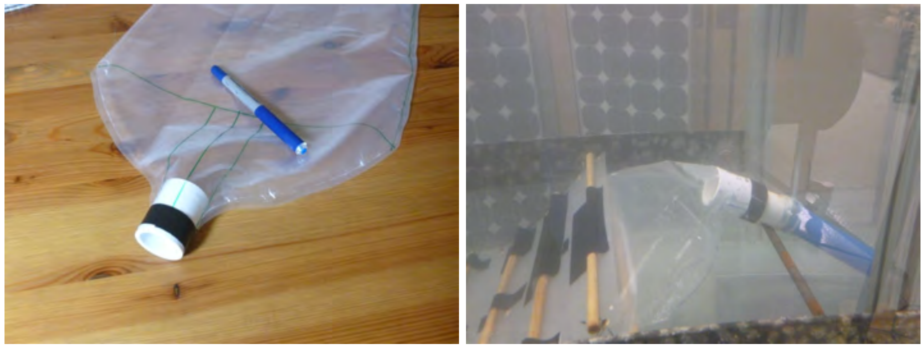

Figure 3.15: Internal membrane configuration including the 3/4*in* PVC coupling fitting as the outlet (*left*) and connection of the CPR valve and outlet pipe (*right*) on Prototype 2.

experiments had the same general configuration: first, the plastic was wrapped around to create only one side sealed by heat, second, the outlet was sealed as an *S-Shape* to improve the flow pattern and reduce head losses, and third, the end of the membrane was made to exactly hold the 3/4*in* PVC coupling fitting. The width of this membrane is 26.5*cm* and the length is determine by the polypropylene sheets. From Figure 3.15 right, the outlet is composed of the check valve and a flexible clear tubing as outlet pipe. The side bars, the aluminum frame, the string material, and the separation between the strings on the ribbon and on the side bars are held constant.

Table 3.8 presents a general description of the Prototypes from 2.1 to 2.4. The design and material of the tubular membrane was held constant during series $T03$, but the series required changing the internal membrane four times. The separation between ribbons (δ) ranged from 10*mm* to 40*mm* and was controlled by the transversal reinforcement as is seen in Fig. 3.16 (*left*). All the final data was gathered at a constant separation between side bars $W_r = 0.360m$ and water depth $H = 0.370m$. Also, all the prototypes demonstrated good performance with 11 wood dowels (5/16*in* in diameter) as transversal reinforcements.

Table 3.8: Parameters for prototypes 2.1 to 2.4 on series $T03$, separation between ribbons δ, separation between side bars W_r, water depth H, type of reinforcement, outlet conditions and resulting motions.

Prototype	δ (mm)	W_r (m)	H (m)	transversal Reinforcement	Outlet Conditions	Successful oscillations?
2.1	10	0.360	0.370	11 WD	Free, complete plastic pipe plus CPR valve	Yes
2.2	20	0.360	0.370	11 WD	Free, complete plastic pipe plus CPR valve	Yes
2.3	30	0.360	0.370	11 WD	Free, complete plastic pipe plus CPR valve	Yes
2.4	40	0.360	0.370	11 WD	Free, complete plastic pipe plus CPR valve	Yes

3.4.2 Experiments

The third series of experiments, referred to as $T03$, used the $0.80mm$ ($0.03in$) thick ribbons referred to as Prototype 2. For all $T03$ tests, the ribbon was located $15.2cm$ ($6in$) above the bottom of the flume. Table 3.9 presents a summary of the experiments executed for series $T03$.

In Tests $T03P2.2-1$ and $T03P2.2-2$, corresponding to Prototype 2.2 ($\delta = 20mm$), the mechanism was tested for two separation distances between side bars: $0.45m$ and $0.36m$, with each string adjusted to have a fixed length of $3in$. 11 acrylic dowels ($3.6mmOD$) were included as transversal reinforcement. Based on these two tests, it was concluded that a fixed length for the strings will not induce oscillations within the pump, and as a consequence, the strings of later prototypes were adjusted with variable lengths to induce the sine wave and its oscillation. From $T03P2.2-3$ it was concluded that the wood dowels performed better than the acrylic dowels (Fig. 3.16 *left*) since they provide better rigidity. In this test the acrylic dowels did not resist the pressure building up inside the membrane, and as a result of this the ribbons tend to deform laterally, causing slow oscillations. Test $T03P2.2-4$ was an attempt to prove the ability of a thicker ribbon to withstand the pressure build up within the membrane by providing the mechanism with more tension on the strings and not using the transversal reinforcements. This test showed that with this thickness the bulging effect at the entrance will cause the oscillations to die immediately if they are induce by hand, and to not appear if the mechanism is not externally disturb.

Tests $T03P2.1$ to $T03P2.4$ resulted in successful oscillations allowing us to gather data for the analysis of δ. The separation between ribbons was changed from $\delta = 10mm$ to $\delta = 40mm$, and the separation between side bars W_r, water depth h, type of reinforcement, and outlet conditions were kept constant throughout the tests. It is important to clarify that the way to control δ was provided by a string attached to the wood dowels (Fig. 3.16 *right*). The spacing between ribbons, δ, was measured between the two inner sides of the plastic sheets.

As in previous prototypes, to determine frequency and amplitude of the ribbon motions, the ADV was located at midlength of the ribbon pump, at the flume's center-line, to acquire distances from the probe head to the ribbon surface (Fig. 3.17 *left*). The flow studies for these prototypes ranged from $0.59m/s$ to $0.76m/s$, set by running both recirculating pumps at frequencies from $30Hz$ to $40Hz$. The frequency spectra (Fig. 3.17 *right*) showed herein as an example,

Table 3.9: Parameters for experiment series $T03$, string length l, separation between ribbons δ, separation between side bars W_r, water depth H, type of reinforcement, outlet conditions and resulting motions.

Test	l (in)	δ (mm)	W_r (m)	H (m)	transversal Reinforcement	Outlet Conditions	Successful oscillations?
$T03P2.2-1$	3.0	20	0.450	0.370	11 AD	Free, complete plastic pipe plus CPR valve	No
$T03P2.2-2$	3.0	20	0.360	0.370	11 AD	Free, complete plastic pipe plus CPR valve	No
$T03P2.2-3$	Variable	20	0.360	0.370	11 AD	Free, complete plastic pipe plus CPR valve	Slow movement
$T03P2.2-4$	Variable	Variable	0.360	0.370	None	Free, complete plastic pipe plus CPR valve	No
$T03P2.1$	Variable	10	0.360	0.370	11 WD	Free, complete plastic pipe plus CPR valve	Yes
$T03P2.2$	Variable	20	0.360	0.370	11 WD	Free, complete plastic pipe plus CPR valve	Yes
$T03P2.3$	Variable	30	0.360	0.370	11 WD	Free, complete plastic pipe plus CPR valve	Yes
$T03P2.4$	Variable	40	0.360	0.370	11 WD	Free, complete plastic pipe plus CPR valve	Yes

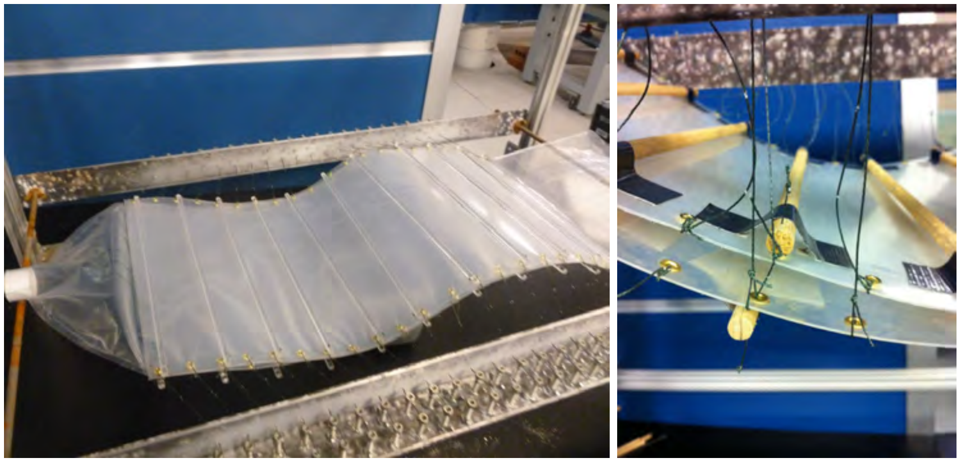

Figure 3.16: Acrylic dowels (*left*) and wood dowels and string connections (*right*) for Prototype 2.

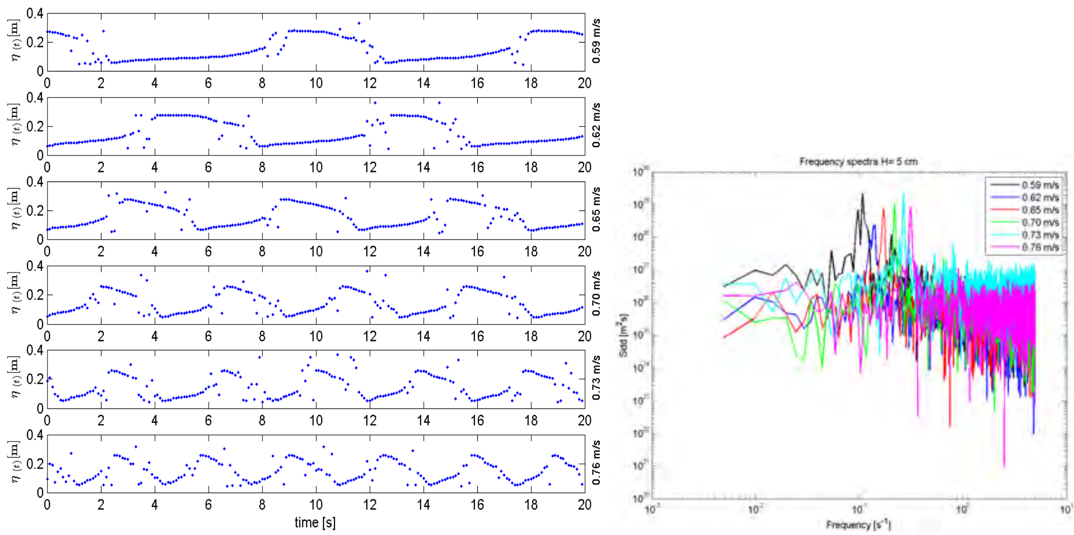

Figure 3.17: Displacement (*left*) and frequency spectra (*right*) measured for Prototype 2.1 from $u = 0.59m/s$ to $u = 0.79m/s$ at a water lift $h = 5cm$.

presents the frequency peaks at which the ribbon was oscillating in each flow speed.

3.5 Prototype 3 Series $T04$

This final section details the changes made in the prototype to understand the influence of changing the material and design of the internal membrane, the width of the ribbons, and the outlet design.

3.5.1 Description

Prototype 3 has the ribbons made of polypropylene copolymer (Plastics International, MN, USA), with physical and mechanical properties presented in Table 3.1. Each ribbon is 0.60*m* (23.6*in*) long, with variable width, and thickness of 0.50*mm* (0.02*in*) for test series $T04$. As in series $T03$, 1/8*in* ID copper grommets (eyelet) by METALgrommets.com where pierced through the holes where each string is tied to the ribbon.

The tubular membrane for Series $T04$ is a polyethylene sheet 0.00076*in* (0.019*mm*) thick, material coming from trash bags by Vasco Brands Inc. As can be seen in Fig. 3.18 (*left*), an impulse sealer was used to create the desired form of the plastic bag. The maximum length of the seal provided by the machine was 20*cm* by 3*mm* as can be seen in Fig. 3.18 (*right*), and since the sealer only provided a straight line, the bottle neck shape with a smooth transition to the outlet feature in Prototype 2 is not provided in this series. Instead, a gradual transition is created for all the prototypes. As can be seen in Table 3.1 and Figure 3.18 (middle), a triangular extension of 10*cm* is provided for prototypes 3.0 and 3.1, and 2*cm* for the rests of series 3.

The outlet in the tubular membrane for all the cases had a circumference of

Figure 3.18: Internal membrane configuration for prototype 3: 20*cm* long impulse sealer (*left*); general aspect of the internal membrane, showing 10*cm* extension after the ribbon ends (*middle*); close-up to the 3mm seal (*right*).

56*mm*. For Prototypes 3.0 to 3.1b the outlet (Fig. 3.19 *left*) was held between the CPR valve already described and the machined PVC ring shown previously in Fig. 3.10. In addition to this, a non permanent, water proof RTV sealant (Silicon Rubber Adhesive Sealant, Translucent RTV 108 by General Electric Co.) and a Schedule 40 $^3/_4$*in* PVC pipe was attached to complete the outlet seal. For the rest of the prototypes in Series $T04$ the CPR valve is introduced in the tubular outlet, held with two to three plastic cable ties and secured with the RTV sealant as shown in Fig. 3.19 (*right*).

Table 3.10 presents a general description of the Prototypes from 3.0 to 3.4. The design of the tubular membrane changed throughout the experiments as required. First, in prototype 3.0 a veterinary glove already described was used, then the custom made polypropylene bags were implemented varying in size as the ribbon width was changed. Additionally, the outlet extension featured in the previous versions was reduced to 2*cm*. The separation between ribbons (δ) started with 10*mm* for prototype 3.0 but was changed and held constant at 5*mm* for all the remaining prototypes. As was the case for Prototype 2, this separation was controlled by the wood dowels ($^5/_{16}in$ in diameter) used as transversal reinforcement. Since the objective of series $T04$ was to understand the influence of the width of the ribbons (W), this geometrical aspect as well as the separation between side bars (W_r) were changed as shown in the table. All the final data was gathered at a water depth $H = 0.370m$. An important thing to highlight is that for Prototype 3.4 the difference between the side bars (W_r) and the width of the ribbon (W) is $5cm$, $1cm$ less than all the previous Prototypes. This was due to the width limitation in the flume, leaving these dimensions as the widest Prototype and separation between side bars. The material of the side bars, the aluminum frame, and the string material remain the same as in Prototype 2 (Series $T03$).

3.5.2 Experiments

The fourth series of experiments, referred to as $T04$, used the $0.50mm$ ($0.02in$) thick ribbons from Prototype 3. For all $T04$ tests, the mean position of the ribbon was located $15.2cm$ ($6in$) above the bottom of the flume. Table 3.11 presents a summary of the experiments executed for series $T04$. The general purpose of this series of experiments is to understand the influence on flow-rate delivered in terms of width of the plastic ribbon.

Test $T4.0$ was conceived to understand the importance of the internal membrane. In previous prototypes the membrane was constrained by poor seals: either the use of a heavy duty duct tape or sealing by heat from an iron which provided uneven seals and small holes. For this experiment a veterinary glove was again used to provide a case to compare the new configuration with previ-

Table 3.10: Parameters for prototypes 3.1 to 3.4 in series $T04$, separation between ribbons δ, separation between side bars W_r, water depth H, type of reinforcement, outlet conditions and resulting motions.

Prototype	δ (mm)	W (m)	W_r (m)	H (m)	transversal Reinforcement	Outlet Conditions
3.0	10	0.30	0.360	0.370	11 WD	Free, complete plastic pipe plus CPR valve. Veterinary glove.
3.1	10 & 5	0.30	0.360	0.370	11 WD	Free, complete plastic pipe plus CPR valve. Polypropylene bag 10 cm extension.
3.1b	5	0.30	0.360	0.370	11 WD	Free, complete plastic pipe plus CPR valve. Polypropylene bag 2 cm extension.
3.2	5	0.35	0.410	0.370	11 WD	Free, complete plastic pipe plus CPR valve. Polypropylene bag 2 cm extension.
3.3	5	0.40	0.460	0.370	11 WD	Free, complete plastic pipe plus CPR valve. Polypropylene bag 2 cm extension.
3.4	5	0.44	0.490	0.370	11 WD	Free, complete plastic pipe plus CPR valve. Polypropylene bag 2 cm extension.

ous tests. Then, using an impulse sealerer, a custom made internal membrane was produced featuring a $3mm$ seal for test $T4.1$ to $T4.4$. $T4.1$ (Prototype 3.1) was built to initially test the custom made membrane, and $T4.1b$ was used to compare the influence of the extension in this membrane. As will be seen in the results (Section 4.1.9) a better performance is given with the $2cm$ extension in $T4.1b$. As a consequence, all the remaining tests in series $T04$ included an extension of 2cm (Fig. 3.19).

In order to define the final separation between ribbons δ, a qualitative tracer test was conducted. Prototype 3.1 ($T4.1$) was not performing efficiently with $\delta = 10mm$. A red dye was injected at the entrance of the prototype to understand how Prototype 3.1 was transporting the water downstream. With a separation of $\delta = 10mm$ the red dye enters the internal membrane with the first half of the ribbon in the upper position (crest, Fig. 3.20 *left*). Theoretically, a seal between the upper ribbon and the lower ribbon is created, which travels downstream as the crest transforms into a trough. For $\delta = 10mm$ a major part of this injected dye injected comes back out during the phase change of the ribbon, demonstrating that the seal is not complete and supporting findings that by increasing δ the performance is decreased (Fig. 3.20 *middle*). In Fig. 3.20 (*right*) it can be seen how the tracer is washed out above the prototype by the mean flow. Due to these results, for all remaining $T04$ experiments, the separation between ribbons was set to $\delta = 5mm$. At this separation, the dye test was also performed, and even if 100% of the dye was not transported by the seal traveling downstream, the qualitative size of the cloud coming out of the ribbon is smaller for $\delta = 5mm$ than for $\delta = 10mm$.

On the other hand, the process of tuning the prototypes and adjusting the different variables is shown in the number of tests required for maximizing a specific Prototype. As will be seen in sections 4.1.10, 4.1.11, and 4.1.12, the correct tensioning of specific strings, the adjustment of the transversal reinforcement, the aperture of the inlet and the correct positioning of the outlet and outlet pipe are critical to achieving a maximum volume of water delivered. Prototype 3.2 required 4 tests ($T4.2a$ to $T4.2d$), while Prototype 3.3 required 3 ($T4.3a$ to $T4.3c$), and even with three iterations performed for Prototype 3.4 ($T4.4a$ to $T4.4c$) the optimal flow rate was not achieved.

Test $T4.2a$ was conducted right after the Prototype was built. As will be seen in section 4.1.10, the results of $T4.2a$ are affected by the rigidity of the strings. Even if the spectra fiber is designed not to absorb water, after 24 hours of placing the prototype underwater the fibers increase their flexibility allowing the ribbons to oscillate better. In the same way, at the end of $T4.2a$ the 2nd and 3rd to last transversal reinforcement demonstrate problems in holding their place with the consequence that they did not work appropriately for the major part of the test. Test $T4.2b$ was not as evident as its predecessor. After finishing this test the only possible variable affecting the performance was the outlet, which was changed and resealed for subsequent tests. Test $T4.2c$ suffered at the conclusion problems with the first two upper strings, which were changed and adjusted for $T4.2d$. Again, as will be seen in section 4.1.10, the results of $T4.2d$ were considered optimal for this configuration. Even with this success an additional test was considered before performing the final series reported. A chamber was created (Fig. 3.21) by releasing the upper and lower transversal reinforcement to provide an additional volume of water in Prototype 3.2. It was theorized that with this flexibility provided, this volume of water was going to be created when the rear part of the ribbon was in the upper position, or forming a crest, and once the device oscillated and the crest transitioned into a trough, the water contained within the chamber would be transported downstream and lifted trough the outlet pipe. As expected and as seen in Fig. 3.21 the chamber was created but the volume of water was not properly transported downstream. The presence of the chamber changed completely the oscillation pattern of the ribbon, creating more resistance and reducing the frequency of oscillations. As a result, the transversal reinforcement was reposition, the chamber eliminated, and the results of this experiment disregarded.

The process of optimization was similar for Test $T4.3a$ to Test $T4.3c$. First, the Prototype was submerged for 24 hours in the flume, and then Test $T4.3a$ was conducted. After this test the four rear string positions were adjusted by reducing the tension. By observation, this configuration was constraining the rear part of the ribbon reducing the frequency of oscillations. After Test $T4.3b$ was concluded, it was evident that the same four positions were too relaxed. As a consequence, for test $T4.3c$ an intermediate tension was provided giving the optimal flow rate for this configuration. On the other hand, the process of optimization for Prototype 3.4 was not successful. After three different tests ($T4.4a$ to $T4.4c$) no significant increase was achieved. Different variables (tension of front and rear strings, and inlet and outlet configuration) were changed to find the optimal flow rate, but as will be seen in section 4.1.12 only an unstable performance was achieved. It is important to highlight that the spacing between side bars is different for all previous prototypes. This was due to space constraints in the flume as previously mentioned, which is hypothesized to affect the general behavior and making the comparison between this prototype and the previous ones not directly applicable.

Table 3.11: Parameters for prototypes 3 on series $T04$, separation between ribbons δ, ribbon width W, separation between side bars W_r, water depth H, type of reinforcement, and outlet conditions.

Test	δ (mm)	W (m)	W_r (m)	H (m)	transversal Reinforcement	Outlet Conditions
$T4.0$	10	0.30	0.360	0.370	11 WD	Veterinary glove.
$T4.1$	10 & 5	0.30	0.360	0.370	11 WD	10 cm extension.
$T4.1b$	5	0.30	0.360	0.370	11 WD	2 cm extension.
$T4.2a$, $T4.2b$, $T4.2c$, and $T4.2d$	5	0.35	0.410	0.370	11 WD	2 cm extension.
$T4.3a$, $T4.3a$, and $T4.3a$	5	0.40	0.460	0.370	11 WD	2 cm extension.
$T4.4a$, $T4.4b$, and $T4.4c$	5	0.44	0.490	0.370	11 WD	2 cm extension.

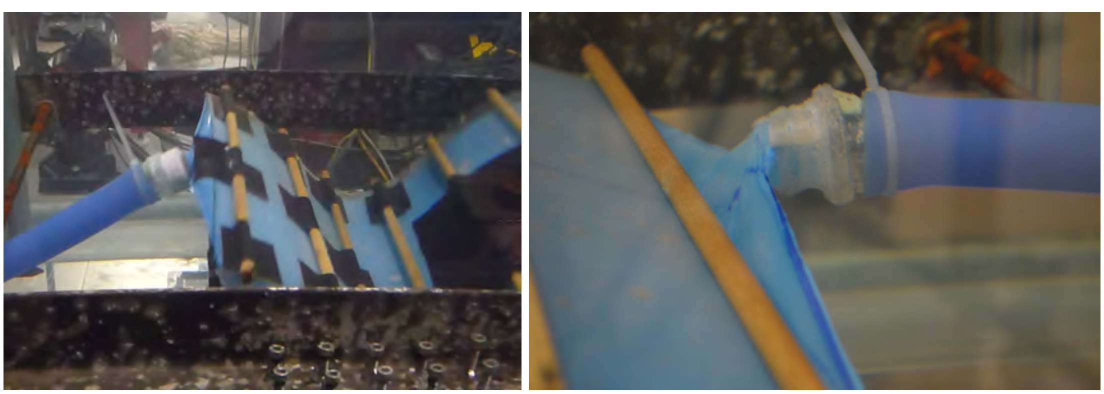

Figure 3.19: Outlet tubing, CPR valve, PVC outlet fittings and $2cm$ extension of test $T04$: Outlet from prototypes 3.0 to 3.1b featuring PVC rings (*left*) and outlet from Prototypes 3.2 to 3.4 featuring plastic cable ties (*right*).

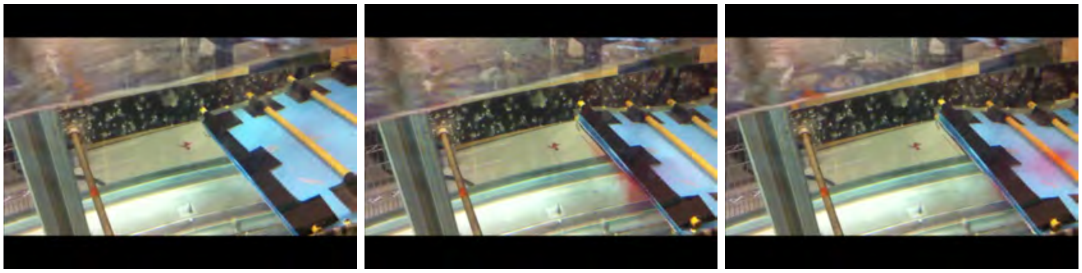

Figure 3.20: Tracer dye injected to characterize the water intake for a spacing between the ribbons $\delta = 10mm$ in prototype 3.0. The three snapshots are not equally spaced in time.

Figure 3.21: Chamber modified by releasing the upper and lower trasversal reinforcement to provide an additional volume of water in Prototype 3.2.

As in previous prototypes, to determine frequency and amplitude of the ribbon motions, the ADV was located at mid length of the ribbon pump, at the flume's center-line. For this series, there was a lot of noise in the distance check mode of the ADV, likely do to the sharpness of the ribbon perturbations. For $T04$ no clean record was possible to achieve. Instead, a velocity record was recorded for each experiment. These data sets were taken at a sampling frequency $f_s = 200Hz$ for $2^{15} \sim 32770$ samples. Fig. 3.22 (*left*) presents the vertical components of one of the velocity records. The flow studies for these prototypes range from $0.43m/s$ to $0.66m/s$, set by running both recirculating pumps at frequencies from $22Hz$ to $34Hz$. The frequency spectra (Fig. 3.22 *right*) showed

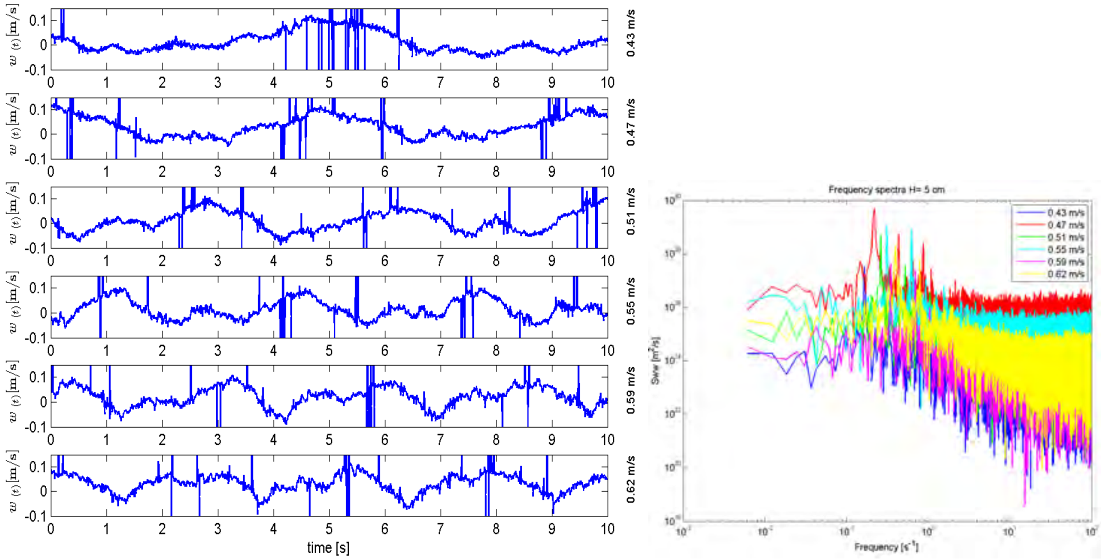

Figure 3.22: Velocity measurements (*left*) and frequency spectra (*right*) measured for Prototype 3.0 from $u = 0.43m/s$ to $u = 0.62m/s$ at a water lift $h = 5cm$.

herein as an example, present the frequency peaks at which the ribbon was oscillating in each flow speed. In order to confirm this frequencies, the spectra from the horizontal velocity component and the second vertical component (the Nortek Vectrino has two independent measurements of the vertical velocity) are used as back up checks.

CHAPTER 4

ANALYSIS OF THE PERFORMANCE OF THE SELF- POWERED PUMP

This chapter presents the results for each experiment, the pump curves for collections of tests performing at different lifting heads, and comments on the design, construction and maintenance aspects of the prototypes. The major part of the information included in this chapter is concerned with the analysis of the results, the understanding of the influence of different components of the device, and the scaling factors of geometrical aspects.

4.1 Pump's response as a function of channel flow rate

4.1.1 Prototype 1.1

As decribed in Table 3.2, $P1.1$ is formed by $0.50mm$ ($0.02in$) thick ribbons, $30cm$ wide and an internal membrane formed with multilayer plastic film. Tests $T01B03$, $T01B04$, and $T01B05$ proved able to transport water through the membrane to the outlet pipe. However, the water level in the outlet pipe presented continuous oscillations that prevented it from actually transporting water. Given the observed behavior of the mechanism, it was suspected oscilations in the rise in water level in the pipe above the free surface level could be due to the stagnation pressure (back pressure) as the water begins to flow backwards towards the internal membrane. However, a quick calculation proved that the observed water level in the outlet pipe exceeded the expected elevation we would get from stagnation pressure alone (i.e., due to the total potential and kinetic energy of the channel flow), so that the additional lift is caused by actual

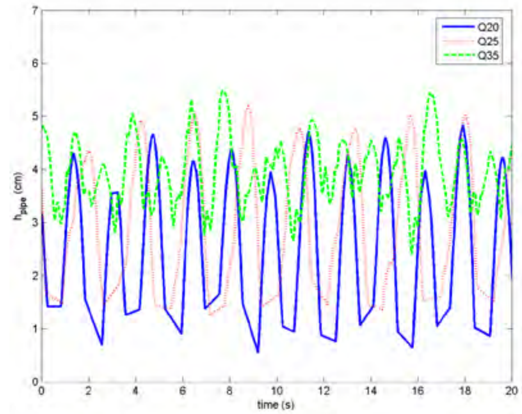

Figure 4.1: Water level inside the outlet pipe (above free surface) for test $T01B05$.

work performed by the ribbon pump.

Images of the water level in the pipe were taken at $30fps$ with a Phantom v9.1 camera (14-bit 1632 x 1200 pixels) for 5 minutes to determine the elevation above the free surface and the period of the observed oscillations in the pipe for each experiment. The time history of three of those tests, for $T01B05$ is presented in Fig. 4.1. The post processing software provided with the camera was used to track the water surface elevation for all the pictures taken.

The measured frequencies of the oscillations in the water level inside the pipe shown in Fig. 4.1 are presented in Table 4.1 , along with the measured frequencies from the ribbon oscillations. The frequencies match for the two highest flow rates, while the frequency of the pipe for the slowest flow is twice that of the ribbon. Although a more detailed analysis is required to study the relationship between the observed oscillations in the pipe's water level, it is evident that they are being forced by the ribbon motions.

Additional tests with the $T01B06$ configuration were conducted adding a check valve to the outlet pipe to minimize any back-flow, resulting in a contin-

Table 4.1: Comparison of the measured frequencies of the ribbon oscillations (f_R) and the oscillations in the water level in the outlet pipe (f_P), for series $T01B05$.

Test	f_R (Hz)	f_P (Hz)
$Q20$	0.303	0.604
$Q25$	0.435	0.438
$Q35$	0.791	0.794

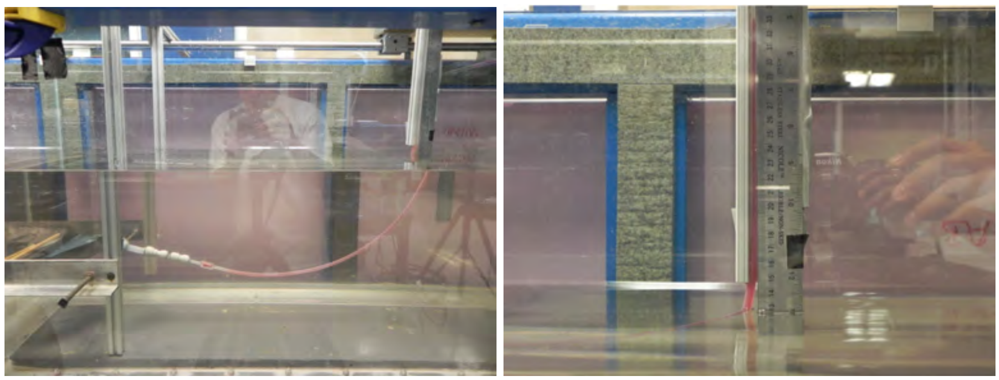

Figure 4.2: Pump head obtained from configuration $T01B05$, $Q25$, using a check-valve to avoid back-flow oscillations.

uous, slow transport of water to a $0.21m$ head (Fig. 4.2). It is important to notice that the addition of contractions and the valve itself added considerable energy losses to the setup, so that a more efficient outlet, with a low-loss check valve will increase the efficiency of the pump.

Based on the outlet configuration described in Section 3.1.2, the following tests (Table 4.2) were conducted to find the pump curves. Five flume speeds were considered and represented by the frequency of the flume's two centrifugal pumps, ranging from $25Hz$ to $35Hz$. For each of the five flume speeds, three water lifts by the pump were considered. The water lift h was measure from the water surface in stagnant conditions to the lowest internal wall of the outlet

Table 4.2: Tests conducted for Prototype 1.1 under different pump frequencies f_{Pump}, water velocities v, water head h and water depth H.

Test	No. of Pumps	f_{pump} (Hz)	v (m/s)	h $(5cm)$ Successful Pumping?	h $(10cm)$ Successful Pumping?	h $(15cm)$ Successful Pumping?	H (m)
$Q25$	2	25.0	0.506	Yes	No	No	0.370
$Q27$	2	27.5	0.564	Yes	Yes	No	0.370
$Q30$	2	30.0	0.604	Yes	Yes	No	0.370
$Q32$	2	32.5	0.642	Yes	Yes	No	0.370
$Q35$	2	35.0	0.694	Yes	Yes	No	0.370

pipe. At a water head $h = 10cm$ there were successful oscillations in all cases but no generated flow rate at the lowest flume speed. The same behavior occurred at a water lift of $h = 15cm$, where oscillations were always present, but pumping did not occurred for any case.

Fig. 4.3 (*left*) presents the flow rates obtained from the pump for the experiments in Table 4.2. As expected, at higher water lifts there is less volume lifted. The maximum flow rate at $h = 5cm$ is approximately $3.6L/h$ while at $h = 10cm$ it is $1.4L/h$. Regardless of the differences between the two cases, the maximum flow rate requires improvements for real applications. In this prototype the outlet presents constant leakage and continuous decay of performance throughout the experiments. The use of heavy duty duct tape as shown in Fig. 3.5 was a temporal configuration and required further refinement in later prototypes. On the other hand Fig. 4.3 (*left*) also shows a variability in the shape of the possible function describing the relationship between flow rate and flume velocity. This situation can be explained by the fact that from one test to the other (e.g.,

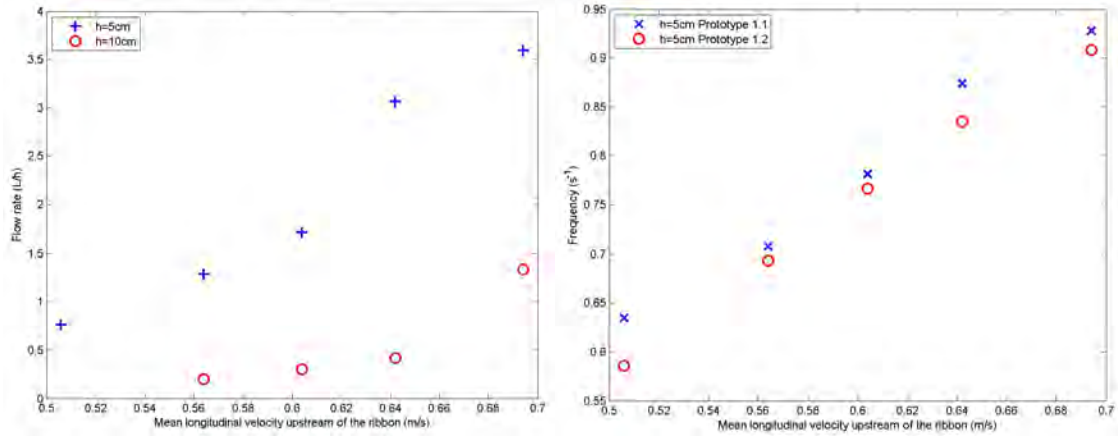

Figure 4.3: Flow rate vs. water speed (*left*) and ribbon frequency vs. water speed for Prototype 1.1 (*right*).

from $0.56m/s$ to $0.69m/s$) 2 to 5 string were required to be replaced, changing the tension in the strings and in that way, the configuration of the ribbon.

Despite the changes in the tension caused by replacing strings, Fig. 4.3 (*right*) shows that from one water lift to the other, the frequency of oscillations remains almost the same at a given flume speed. This means that the oscillations of the ribbon are not being affected either by the water lift or by the change of the strings in each test.

4.1.2 Prototype 1.2

As decribed in Table 3.3 Prototype 1.2 is formed by $0.50mm$ ($0.02in$) thick ribbons, $30cm$ wide and an internal membrane formed with a $0.004in$ ($0.11mm$) thick polyethylene sleeve. The experiments described in Table 4.3 were run with the configuration presented in Section 3.2. As in the previous prototypes, five flume speeds were considered and represented by the frequency of the flume's two centrifugal pumps, ranging from $25Hz$ to $35Hz$. For each of the five flume

Table 4.3: Tests conducted for Prototype 1.2 under different pump frequencies f_{Pump}, water velocities v, water head h and water depth H.

Test	No. of Pumps	f_{pump} (Hz)	v (m/s)	h $(5cm)$ Successful Pumping?	h $(10cm)$ Successful Pumping?	h $(15cm)$ Successful Pumping?	H (m)
$Q25$	2	25.0	0.506	Yes	Yes	No	0.370
$Q27$	2	27.5	0.564	Yes	Yes	No	0.370
$Q30$	2	30.0	0.604	Yes	Yes	Yes	0.370
$Q32$	2	32.5	0.642	Yes	Yes	Yes	0.370
$Q35$	2	35.0	0.694	Yes	Yes	Yes	0.370

speeds, three water lifts were considered. From Table 4.3 it can be seen that the change of the internal membrane from the diper bag to the veterinary glove improved the performance of the pump. Pumping was not successful for the two lowest flume speed cases for a water lift of $h = 15cm$. The veterinary glove provided an easy way to attached the outlet pipe and a more reliable configuration with a better seal between internal membrane and outlet pipe.

Fig. 4.4 (*left*) presents the flow rate obtained from the pump for the experiments in Table 4.3. The maximum flow rate at $h = 5cm$ is approximately $13.2L/h$, showing that an important increase in performance was obtained. Despite the increase in performance the maximum flow rate still requires improvements for real applications. In this prototype the internal membrane did not cover the whole width of the ribbon as can be seen in Fig. 4.5. This reduces the water volume being acted on by the ribbon and is suboptimal.

In contrast to the behavior presented for Prototype 1.1, the frequency of this

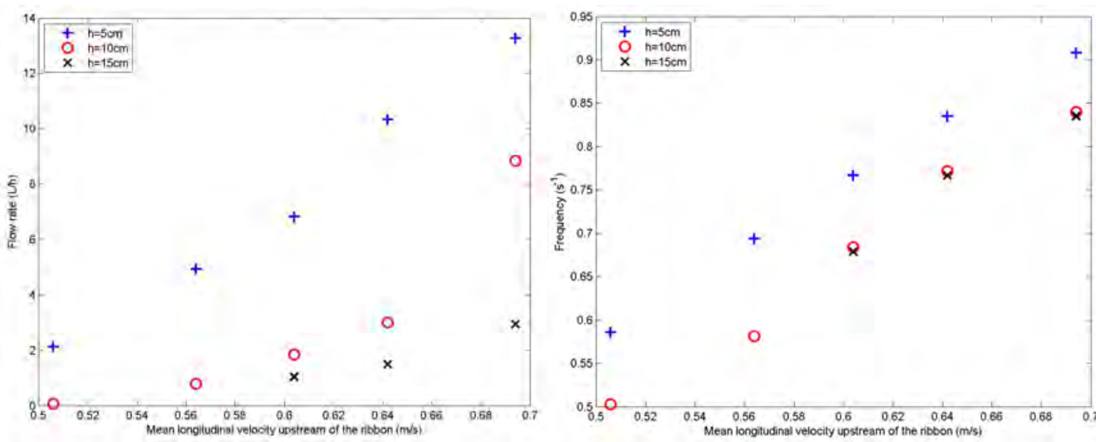

Figure 4.4: Flow rate vs. water speed (*left*) and Ribbon frequency vs. water speed (*right*) for Prototype 1.2.

new configuration presented an appreciable change from one case to the others as can be seen in Fig. 4.4 (*right*) (i.e, from $h = 5cm$ to the other two water lifts). Even if the shift in frequency is less than $0.1s^{-1}$, the data shows that the performance was reduced when the higher water lifts were tested. After $h = 5cm$ was tested, 4 strings were changed in the front of the ribbon (8 in total counting upper and lower ribbons) and 9 in total in the rear. As seen in the figure, changing these strings affected the overall behavior of the ribbon and reduced its performance in terms of oscillations. Despite this change, the flow-rate from Prototype 1.2 shows an important increase in performance (Fig. 4.6 *left*).

Finally, Fig. 4.6 (*right*) shows a comparison of the frequency at different flume speeds for $h = 5cm$ on Prototypes 1.1 and 1.2. The discrepancies between frequency oscillations are less than $0.05s^{-1}$from one prototype to the other. This physically means that, even if the internal membrane was change completely, the consistency in ribbon motion is preserved. On the other hand, the fact that Prototype 1.2 is pumping more water seems to affect slightly the oscillation represented in the figure by the small shift toward lower frequency.

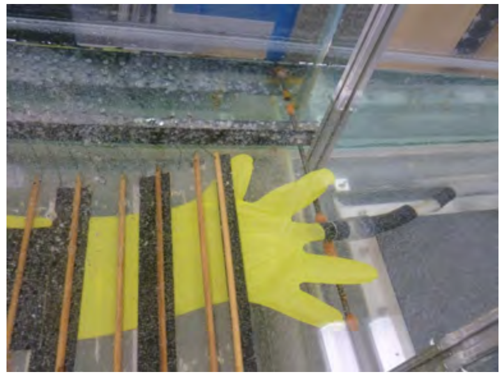

Figure 4.5: Internal membrane in Prototype 1.2.

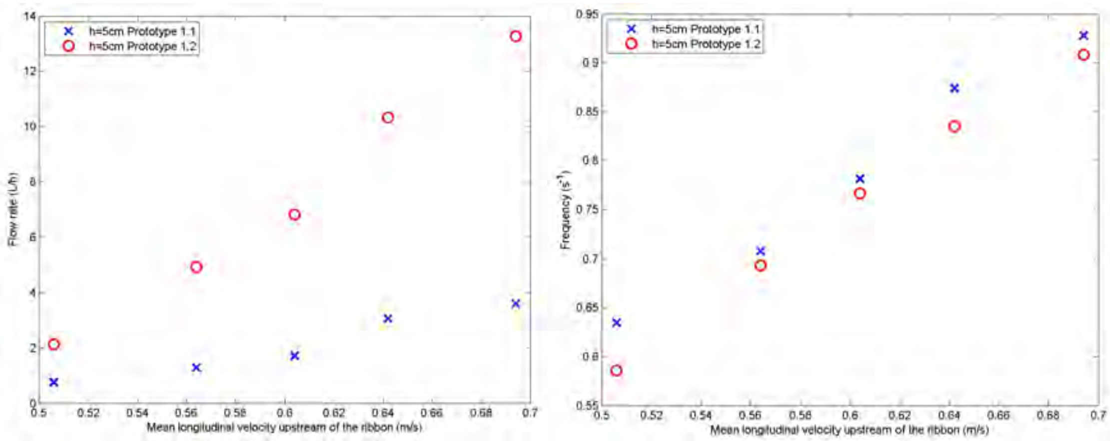

Figure 4.6: Comparison of Prototype 1.1 and 1.2 for flow rate (left) and frequencies (right) at a water lift $h = 5cm$

4.1.3 Prototype 2.1

As described in Table 3.8, Prototype 2.1 has a separation between ribbons $\delta = 10mm$ and a polypropylene thickness of $0.80mm$ ($0.03in$), $30cm$ wide and internal membrane formed with a $0.005in$ ($0.127mm$) thick polyethylene sheet. For all water lifts ($h = 5cm$, $h = 10cm$, $h = 15cm$, $h = 20cm$, $h = 25cm$), the frequency of the flume's recirculating pumps (f_{pump}) varied from $30Hz$ to $40Hz$ on increments of $2Hz$, establishing six tests per lift. Prototype 2.1 was successful in oscillating and pumping water at all of the 30 tests conducted, demonstrating a better resistance to damage at higher speeds. The combination of the grommets and a thicker material prevented the strings from tearing the plastic.

Fig. 4.7 (*left*) shows the mechanism's stability in terms of performance. A linear relationship is expected between the ribbon frequency and stream velocity, which can be seen in the Figure. It is also expected that small changes like replacing a small number of strings will not affect the oscillations, and this is demonstrated by the fact that for the same stream velocity the ribbon will oscillate at the same frequency. Only $h = 10cm$ appears to vary with respect to this tendency. This can be explained by the fact that after finishing the test at $h = 5cm$ the internal membrane was changed due to rupture. On the other hand, the increase in reliability can also be supported by describing that after $h = 10cm$ only 3 strings were repaired, and after $h = 15cm$, $h = 20cm$ and $h = 25cm$ no strings required repairs. Fig. 4.7 (*right*) shows the variability of the amplitude with respect to water speed. For this prototype in particular it seems like the amplitude is reduced as speed increases. Apparently, for this configuration, as the flow speed increases the oscillation is induced earlier and as consequence, the full amplitude is not reached. Another possible explanation is that at lower speeds the ADV picks up more noise, affecting the calculation of the amplitude and biasing the final result.

Fig. 4.7 (*lower*) shows the flow rate that the mechanism generated against different water lifts (h). The first thing to notice is that the results for $h = 5cm$ are affected by a hole in the internal membrane, which was notice after collecting the data. Due to this small rupture the data series will not be taken into account for further analysis. On the other hand, it can be seen that the mechanism requires more energy in the stream to start its oscillations. Previous prototypes

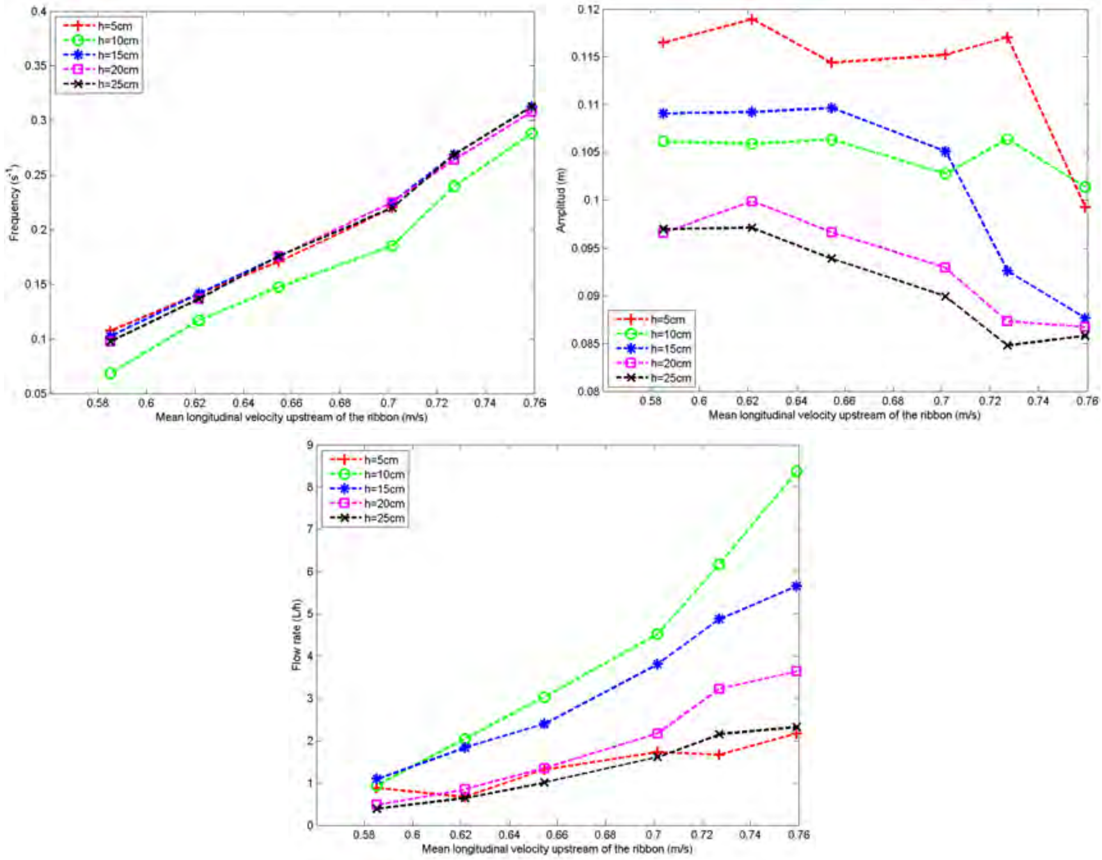

Figure 4.7: Variation of oscillation frequency (*left*), amplitude (*right*) and flow rate (*lower*) as function of water speed (u) for Prototype 2.1.

were tested with $0.51m/s$ as the lowest flume speed. This prototype required an initial speed of $0.58m/s$. From a first comparison with Prototype 1.2 at $h = 10cm$ and $u = 0.58m/s$ the flow rate shows virtually no improvement: they both pump $1L/h$. When $H = 10cm$ and $u = 0.70m/s$ Prototype 1.2 behaves better by pumping $8.7L/h$ versus the $4.5L/h$ pumped by Prototype 2.1. Regardless of these results, it cannot be concluded that by increasing the thickness of the ribbons from $0.02in$ to $0.03in$ decreased the efficiency. There are other factors that affected the performance of Prototype 2 and its $T03$ series of experiments. First, the internal membrane is thicker ($0.127mm$ vs $0.11mm$) affecting both flexibility and the way the internal membrane provides the seal when there is a pinching point. Second, the grommets were added and its influence on the generated flow rate is not clear. They help to increase the resistance to tear but at this stage it is difficult to determine if they are affecting the constrictions created by the ribbons. And last, the outlet was modified completely; in Prototype 2.1 only the PVC coupling, the CPR valve, and the plastic tubing used as outlet pipe were used.

4.1.4 Prototype 2.2

From Table 3.8, Prototype 2.2 has a separation between ribbons $\delta = 20mm$ and a polypropylene thickness of $0.80mm$ ($0.03in$), $30cm$ wide and internal membrane formed with a $0.005in$ ($0.127mm$) thick polyethylene sheet. As in Prototype 2.1, Fig. 4.8 (*left*) shows the mechanism's stability in terms of performance. A linear relationship between flume velocity and oscillation frequency was evident in the test executed for this version. For Prototype 2.2 none of the results showed an unusual behavior which was expected since no major changes were done through the tests. Fig. 4.8 (*right*) shows the variability of the amplitude with respect to water speed. For this prototype in particular it seems that the amplitude increases as speed increases. This will not be concluded since the data gathered had noise that enhances the uncertainty to the point where this conclusion cannot be drawn. Fig. 4.8 (*lower*) shows the flow rate that the mechanism generated against different water lifts (h). The first thing to notice is that the ribbon did not move at any height at a flume speed of $0.58m/s$. This could be explained by the increment in δ from $10mm$ to $20mm$. The mechanism requires more energy to be started, and as consequence a higher flume water speed is expected. From the tests it was also notice that at a speed of $0.62m/s$ the ribbon

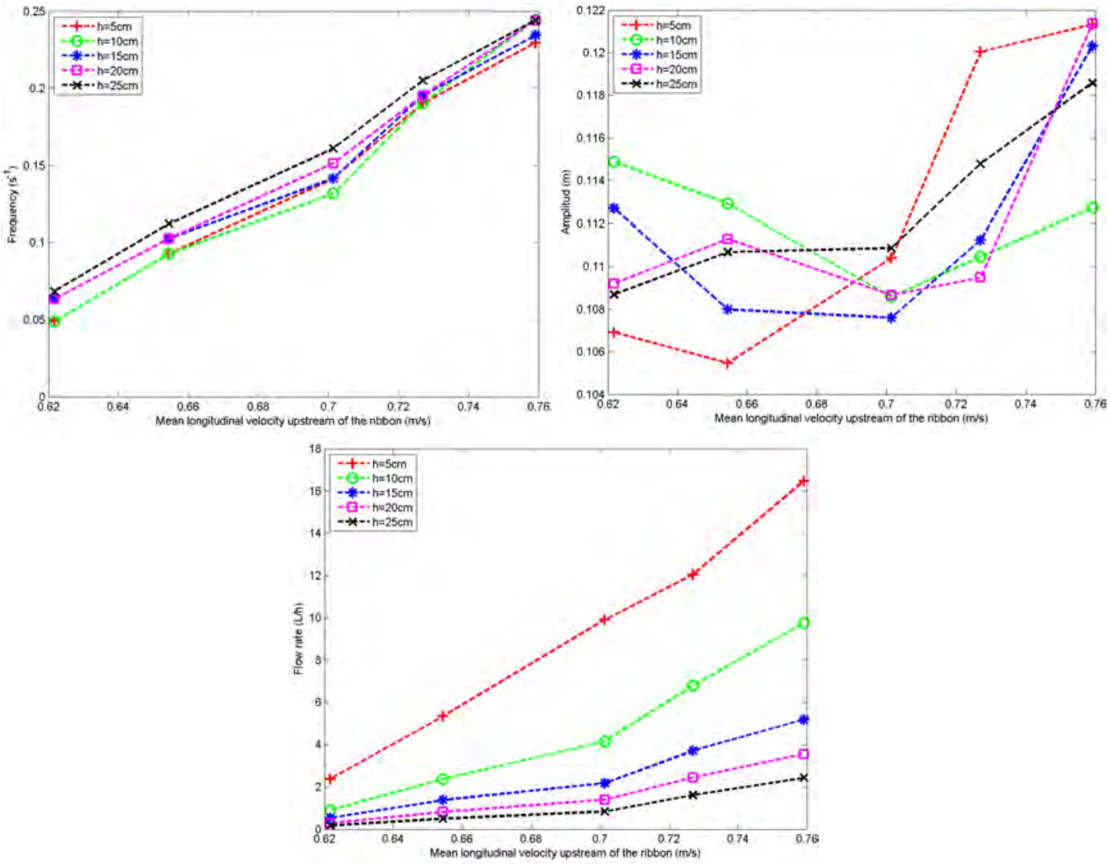

Figure 4.8: Variation of oscillation frequency (*left*), amplitude (*right*) and flow rates (*lower*) as function of water speed (u) for Prototype 2.2.

had slow unstable oscillations for all water lifts, but regardless of this observation the mechanism was able to pump at all heads. By comparing the case when $h = 10cm$ and $u = 0.70m/s$ Prototype 1.2 still behaves better by pumping $8.7L/h$ versus the $4.1L/h$ pumped by Prototype 2.2.

4.1.5 Prototype 2.3

Again, from Table 3.8, Prototype 2.3 has a separation between ribbons $\delta = 30mm$ and a polypropylene thickness of $0.80mm$ ($0.03in$), $30cm$ wide and internal membrane formed with a 0.005*in* (0.127*mm*) thick polyethylene sheet. Prototype 2.3 presented irregular results as can be seen in Fig. 4.9. First, a liner increment in the frequency of oscillation as function of water speed (u) was seen (Fig. 4.9 *left*), but the flow rate showed inconsistencies throughout the experiments (Fig. 4.9 *right*). This prototype was tested after Prototype 2.4, and was the last version of Prototype 2.

The tests began with a water lifts of $h = 5cm$ and the results showed an unstable tendency (frequency vs. water speed). After the first 4 experiments at $h = 5cm$, the last two flow rates changed tendency, creating a local minimum. Due to these results the internal membrane was inspected, and small holes were discovered in the rear of the internal membrane, near to the connection of the PVC coupling (Fig. 4.10 *left*). It was also notice that the internal membrane was supporting most of the pressure from the flow rate and the pumping action at the rear sides of the membrane (Fig. 4.10 *right*). Though the $S - shaped$ outlet provided a better flow field, still the water flow was trying to rip off the seal created for the internal membrane. Based on the holes and the necessity to reinforce the outlet, the membrane was changed. A second result at the same water lift $h = 5cm$ is reported in Fig. 4.9 *left*. This test was conducted with the same configuration plus the new membrane but still the flow rate was less than the one reported for the membrane with holes on it. The bag was rechecked finding no visible defects, and the test for the water lift $h = 10cm$. Based on these two last results it is concluded that the prototype did not maintain the same configuration. Further tests will present completely different results and will not allow conclusions to be drawn in terms of the variability of δ based on the configuration of Prototype 2. It is possible that the tension on the strings changed when the prototype was moved for inspection and when the internal membrane was

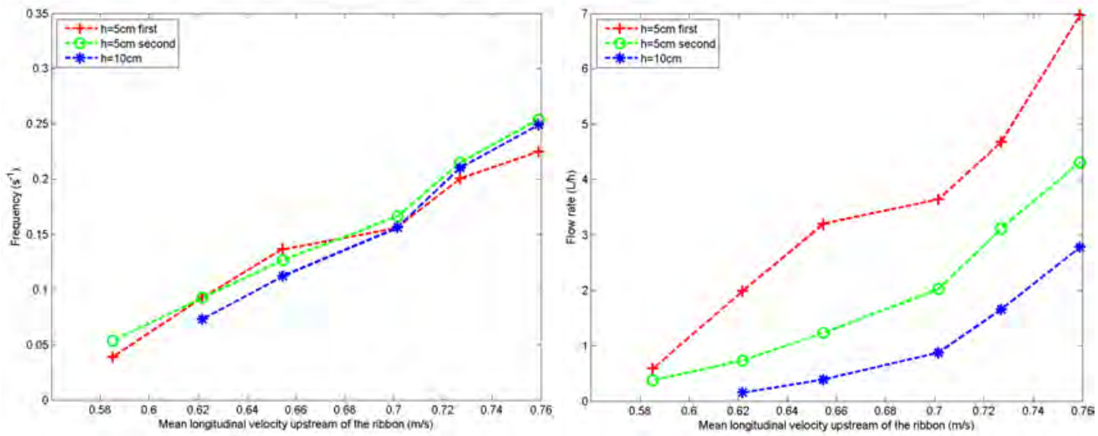

Figure 4.9: Variation of oscillation frequency as function of water speed (u) (*left*) and flow rate as function of water speed (u) and water lifts (h) (*right*) for Prototype 2.3.

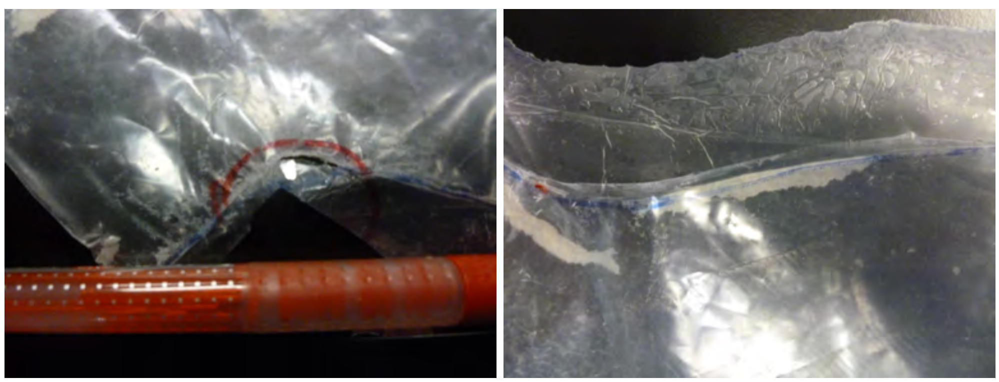

Figure 4.10: Challenges faced by the internal membrane: holes caused by stiffness of the heat seal (*left*) and seal break-down in places where the heat applied was not sufficient (*right*).

replaced. As a consequence, the change in the general configuration led to the decision of terminate test $T03$ at this point.

4.1.6 Prototype 2.4

From Table 3.8, Prototype 2.4 has a separation between ribbons $\delta = 40mm$ and a polypropylene thickness of $0.80mm$ ($0.03in$), $30cm$ wide and internal membrane formed with a $0.005in$ ($0.127mm$) thick polyethylene sheet. Prototype 2.4 was carried out before Prototype 2.3 but reported at this point. In general, this version required more flow energy to be able to start its oscillations. As can be seen in Fig. 4.11 (*left*) the lowest speed tested ($u = 0.58m/s$) induced slow oscillations at all water lift cases, but no water was pumped except for $h = 5cm$. At a flume speed of $u = 0.62m/s$ there were stable oscillations but only significant volume of water pumped at $h = 5cm$ and $10cm$. In the same way, at $u = 0.65m/s$ the mechanism did not pump at $h = 20cm$ and $25cm$. The linear tendency in frequency as function of flume speed remained. Fig. 4.11 (*right*) shows that amplitude presented significant variation over the cases studied. For this version the tendency is similar to that of Prototype 2.1 as the flow speed increases the amplitude tends to reduce. With this, two explanations are possible: either as the flow speed increases the oscillation is induced earlier and as consequence, the full amplitude is not reached, or at lower speeds the ADV picks up more noise, affecting the calculation of the amplitude and deviating the final result. On the other hand, comparing the results of Fig. 4.11 (*lower*) at $h = 10cm$ and $u = 0.58m/s$ there is no volume of water displaced, and at $h = 10cm$ and $u = 0.70m/s$ the flow rate is $2.1L/h$ versus the $8.7L/h$ from Prototype 1.2 or $4.5L/h$ from Prototype 2.1.

A final remark on this prototype is appropriate about the tension in the front and rear strings and the bending effect caused by them. The original design proposed a string length $l = 3in$. It was demonstrated that once the ribbons are operating as a pump and creating the pinching points and constrictions, this

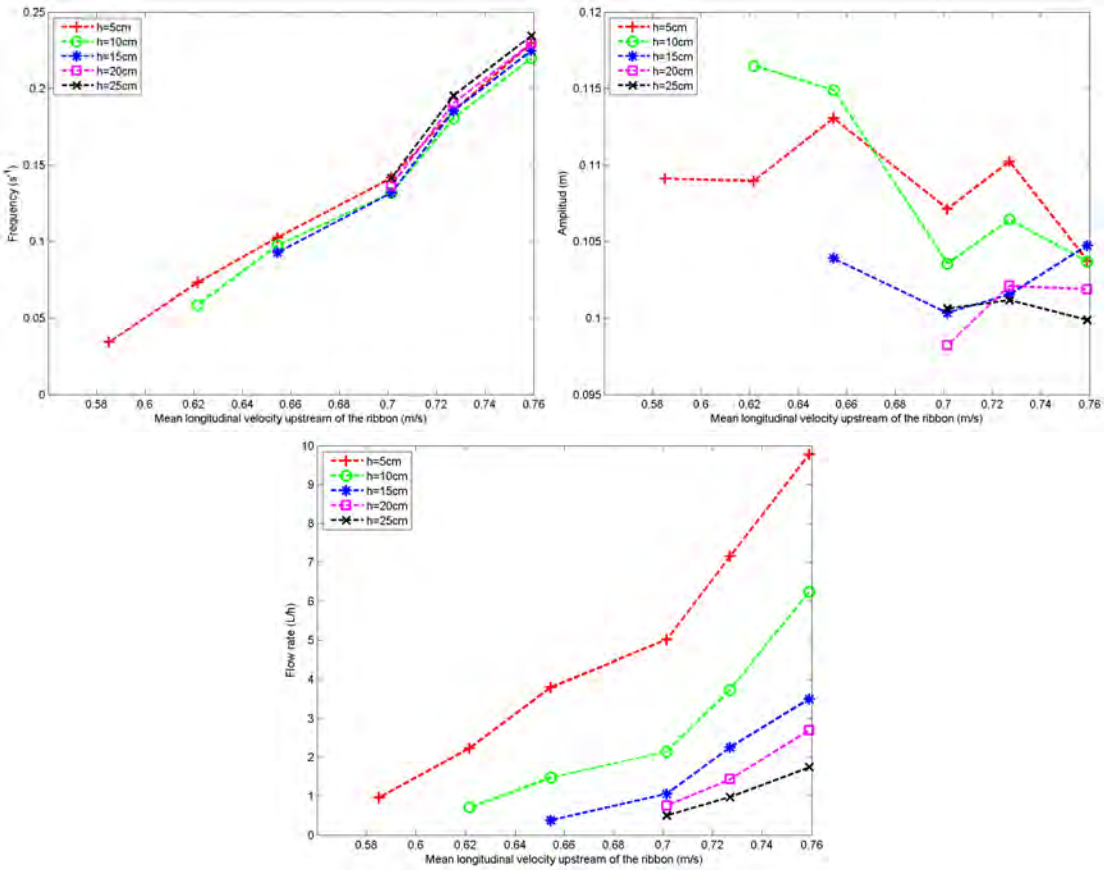

Figure 4.11: Variation of oscillation frequency (*left*), amplitude (*right*) and flow rates (*lower*) as function of water speed (u) for Prototype 2.4.

length does not induce a stable sine wave in the ribbons. Due to this, the length was reduce in the 3 front and 3 rear strings (for both top and bottom ribbons) to $l = 3/4in$, and for all other strings to $l \geq 3in$. By doing this, the spacing between the ribbons δ is controlled in the front and rear areas by the tension on the strings and in the remaining parts by the prescribed δ for the prototype version being tested. Fig. 4.12 presents this effect which is strong in Prototype 2.4 since it was the prototype with the highest δ. Regardless of the transversal reinforcement, the tension of these front strings creates a bulging effect on the ribbon creating a constrained entrance to the mechanism.

Figure 4.12: Constriction at the entrance sides due to the tension on the strings and bulging at the center on Prototype 2.4.

4.1.7 The influence of the ribbon spacing δ in Prototype 2

Fig. 4.13 shows the influence of ribbon spacing (δ) at each water lift (h). Each figure contains the series of data for Prototypes 2.1 ($\delta = 10mm$), 2.2 ($\delta = 20mm$) and 2.4 ($\delta = 40mm$) and presents the flow rate of the mechanism as function of the average channel flow speed. At the top left figure ($h = 5cm$) it is possible to identify a performance problem at $\delta = 10mm$. The expected data series is an almost flat line and the reason for this was identified before (Section 4.1.3) as a rupture in the internal membrane. Taking into account only $\delta = 20mm$ and $\delta = 40mm$ its seems that by increasing the spacing between ribbons the performance of the mechanism is decreased. At $h = 10cm$ the best overall performance is $\delta = 10mm$ except for the two highest flume speeds where $\delta = 20mm$ exceeds the generated flow rate of $\delta = 10mm$. The point of inflection for the data series of $\delta = 10mm$ shows that after conducting the experiment at $u = 0.70m/s$ the performance increased, suggesting that at lower flume speeds more water could have been pumped. In the same way, this suggests that the data series recorded for $\delta = 10mm$ was not completely tuned leading to lower flow rates. From $h = 15cm$, $h = 20cm$ and $h = 25cm$ it can be concluded that increasing the spacing to more than $\delta = 10mm$ decreases the performance of the mechanism. Apparently, the constriction created by the ribbons at higher spacings does not provide enough stagnation for the water to be pumped.

4.1.8 Prototype 3.0

Prototype 3.0 is the base line for comparison with previous prototypes. For this specific case, the general configuration (except for the outlet) is the same as in Prototype 1.2. It is important to clarify that the only thing that is not possible to compare is the strings length and tension, which for both prototypes were variable. As has been previously described the strings restrain the plastic sheets in order to induce a sine wave, which will be permanent but unstable. When the prototype is regarded as having variable string lengths this means that the first and last four strings are less than $3/4in$, and the remaining strings are set as required by the length of the ribbon and the induced amplitude on the material.

Fig. 4.14 *left* shows the mechanism's stability in terms of performance. A straight line tendency between flume speed and oscillation frequency was apparent in the test executed for this version. For Prototype 3.0 none of the results showed an unusual behavior. Fig. 4.14 *right* presents the flow rate that the mechanism pumped to different lifting heads (h). In this case the maximum flow-rate was $6.4L/h$ at a flow speed $u = 0.62m/s$. This upper value was obtained by running the variable frequency pumps from the flume at $34Hz$. Comparing Prototype 3.0 with Prototype 1.2 (Fig. 4.15) we can say that Prototype 1.2 performed slightly better. At low flow rates the behavior is the same but once the average flume speed increases the flow-rate delivered by Prototype 3.0 remains

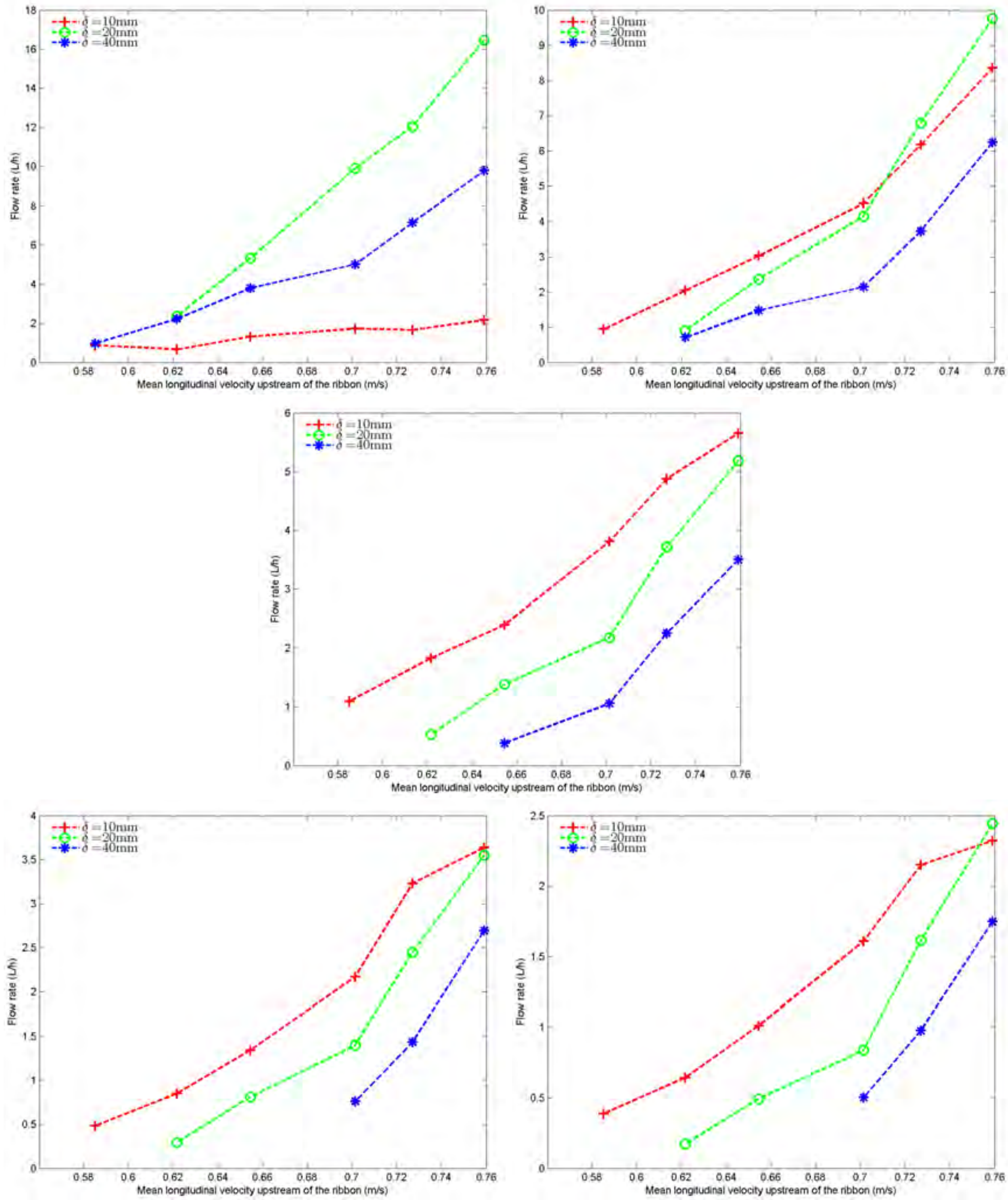

Figure 4.13: Variation of flow rate pumped as function of water flume speed (u) for Prototype 2 from $h = 5cm$ (*top left*) to $h = 25cm$ (*bottom right*).

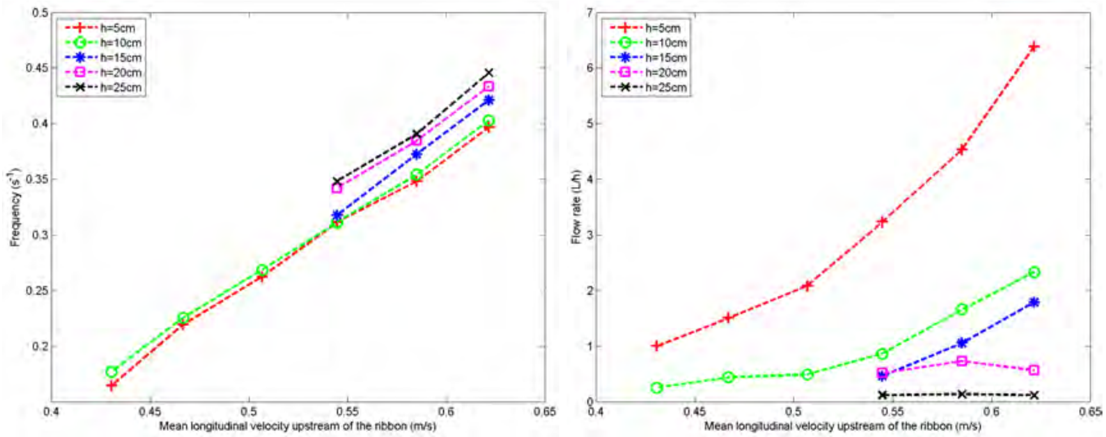

Figure 4.14: Variation of oscillation frequency (*left*), and flow rates (*right*) as function of water speed (u) for Prototype 3.0.

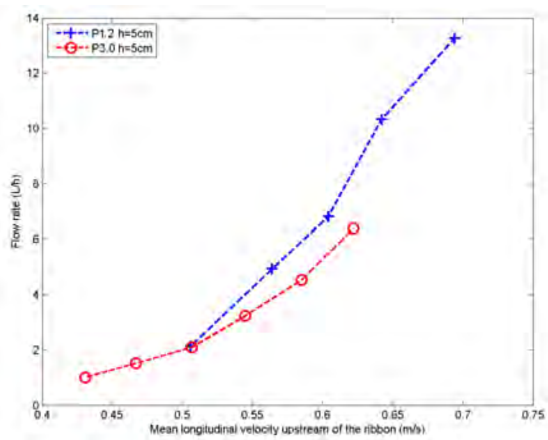

Figure 4.15: Comparison of flow rates as function of water speed (u) for Prototype 1.2 and 3.0.

at a lower level relative to that achieved by Prototype 1.2. Regardless of this results, it is possible to affirm that both prototypes are performing at the level expected. The prototypes configurations are similar but not exactly the same since the tension and length of the strings are not the same, and the outlet pipe and outlet configuration have been changed. Additionally, we can consider that the performance difference is within the uncertainty limits.

4.1.9 Prototype 3.1 and 3.1b

Prototype 3.1 and 3.1b were created to understand the performance of the new internal membrane. With the impulse sealer the membrane is covering the whole length and width of the ribbons, and presents an extension to the outlet in the form of an isosceles triangle. For prototype 3.1 the extension is $10cm$ and for 3.1b the extension is $2cm$.

For Prototype 3.1, Fig. 4.16 (*left*) shows the mechanism's stability in terms of performance. Again, the frequency of oscillation increases as the mean flow increases. For this case, the tendency is not a perfect straight line but it is considered that this variations are withing the uncertainty expected for these tests. In terms of frequencies, P3.1 oscillates faster than P3.0. For example, at $0.43m/s$ the former oscillates at $0.22Hz$, while the later does it at $0.17Hz$. In the same way, at $0.62m/s$ P3.1 oscillates at $0.54Hz$ while P3.0 does it at $0.40Hz$. Fig. 4.16 (*right*) shows the volume of water pumped as a function of the flume mean flow velocity. With this information, P3.1 performs better than P3.0 except for two cases. At a lift of $h = 5cm$ and a flow speed $0.43m/s$ P3.1 delivered $0.67L/h$ in contrast to the $1.00L/h$ delivered by P3.0. In the same way at a lift of $h = 5cm$ and a flow speed of $0.47m/s$ P3.1 delivered $1.16L/h$ in contrast to the $1.51L/h$ delivered by P3.0. For all the remaining cases, Prototype 3.1 performs better in terms of flow rate delivered at any given water lift.

Fig. 4.17 shows the results for prototype 3.1b. The objective was to understand the influence of the extension on the flow rate delivered and the frequency of oscillation. At $h = 5cm$ this has been the most efficient of all prototypes. At the nominal velocity of $65cm/s$ we obtained a flow rate of $20.8L/h$. The additional trends for $h = 10cm$ to $h = 25cm$ were not tested since the performance

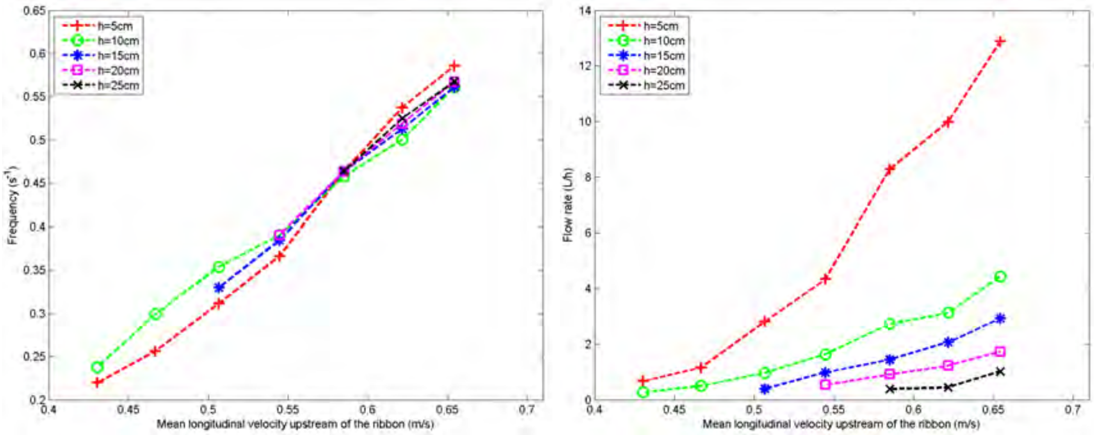

Figure 4.16: Variation of oscillation frequency (*left*), and flow rates (*right*) as function of water speed (u) for Prototype 3.1.

of the prototype started to decay. All the strings were checked and no apparent malfunction was detected. A hypothesis for this degradation is the existance of a hole or defect in the internal membrane not visible at the moment of performing the check-up after the test was conducted. Apparently, additional stress is induced in the joint between the CPR valve and the plastic membrane. Since the CPR valve and the fittings attaching it to the internal membrane are closer to the prototype, they are subject to more frequent and stronger movements. As a consequence, this type of outlet configuration in the internal membrane is more efficient in terms of transporting water but less reliable in duration. At this point it is considered that this situation is not a concern since the plastic material used for building the membrane came from common materials such as a trash bag.

Fig. 4.18 presents a comparison among Prototypes 1.2, 3.0, 3.1 and 3.1b. The idea was to understand the performance of the new internal membrane created with the impulse sealer relative to the already tested cases which had similar design conditions. As can be seen from this Figure, Prototype 3.1b presents the

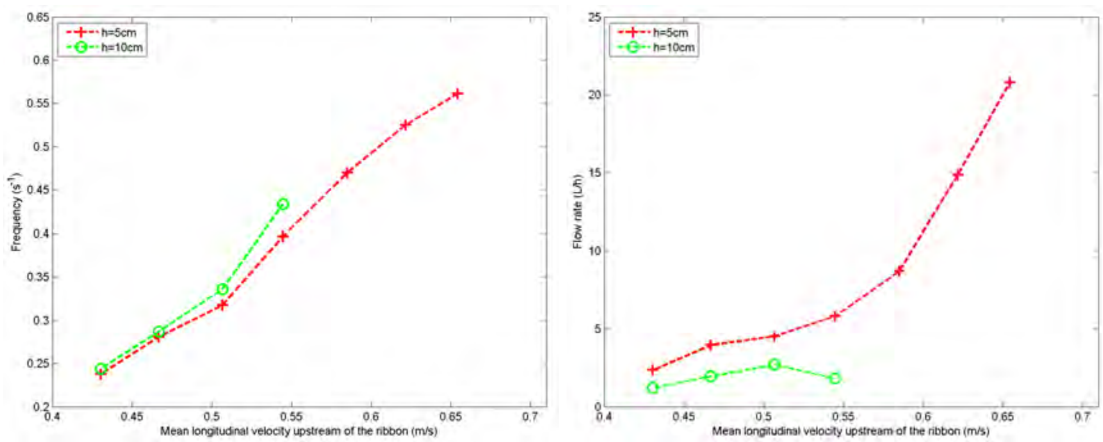

Figure 4.17: Variation of oscillation frequency (*left*), and flow rates (*right*) as function of water speed (u) for Prototype 3.1b.

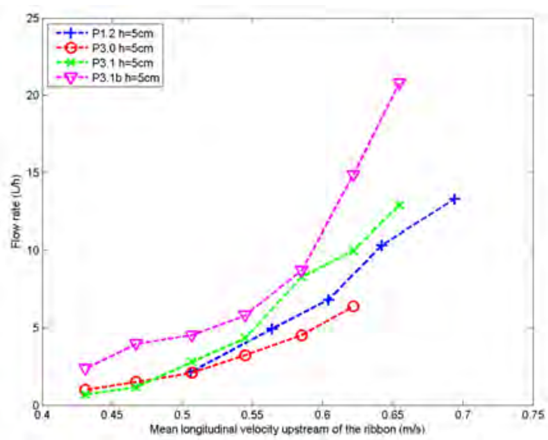

Figure 4.18: Comparison of flow rates as function of water speed (u) for Prototype 1.3, 3.0, 3.1 and 3.1b.

best behavior of all 4 prototypes. In the low velocity ranges the difference is no more than $2L/h$, but for the last two nominal velocities tested the difference is considerable. Prototype 3.1b delivers $20.8L/h$ at a flow rate of $0.65m/s$ while the previous maximum flow rate was seen in Prototype 1.2 with $13.2L/h$ at $0.69m/s$.

A test to find the shut-off head for the configuration of Prototype 3.1b was conducted and its results shown in Fig. 4.19. The pump curves will not be presented since the different lifting heads h were not tested due to the decay in performance as previously described. As a consequence, the interpretation of the shut-off head must be given by direct measurements. A simple test running the flume at a certain speed and the outlet pipe vertically positioned provided information for the evolution of the water column above the free surface through time. The first thing to notice from these results conducted at two different speeds is that the performance of the prototype decays rapidly and the data gather is not consistent. Each series spans around 40 minutes, enough time for several strings to fail and release transversal reinforcements. Since the test can not be stopped to repair the prototype, all the results are affected by the decay in performance during each experiment. For this reason , we can see that the initial tendency for $0.76 m/s$ is higher to the tendency shown by $0.70 m/s$, but sometime around the fifth minute the performance decays suddenly and both tendencies indicate the same shut-off head. Based on this interpretation, a reading of 23 cm for a speed of $0.70 m/s$ could be given as a first approximation, considering this data point was affected by performance. Additionally, it is not possible to give a first approximation for the second speed since the strings and transversal reinforcement were affected in the early portions of the test.

4.1.10 Prototype 3.2

As described in Table 3.10, Prototype 3.2 has a polypropylene thickness of $0.50mm$ ($0.02in$), a $0.00076in$ ($0.019mm$) thick internal membrane with a $3mm$ seal and $2cm$ of extension , the CPR valve as a check valve, separation between ribbons $\delta = 5mm$, and width W of $35cm$. For all water lifts ($h = 5cm$, $h = 10cm$, $h = 15cm$, $h = 20cm$), the frequency of the flume's recirculating pumps (f_{pump}) varied from $22Hz$ to $34Hz$ in increments of $2Hz$, establishing seven tests per lift

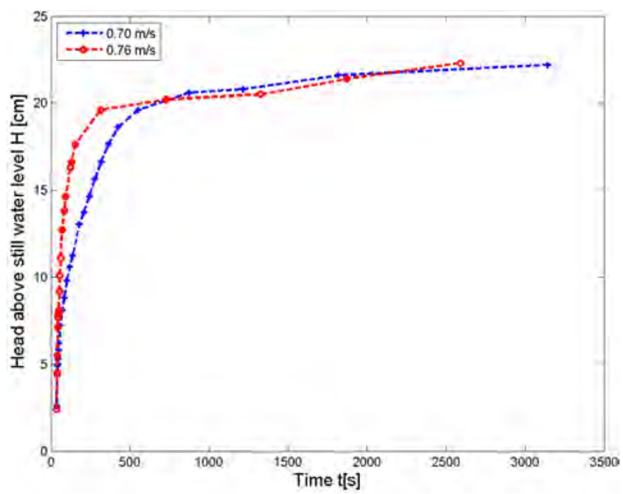

Figure 4.19: Shut-off head results for Prototype 3.1b.

to be overcome. Prototype 3.2 successfully oscillated at all of the 28 tests conducted and pumped water at 25 of the 28 tests (the exceptions were the lowest flow speed at $h = 15cm$ and the two lowest speeds at $h = 20cm$), showing a better performance in terms of flow rate at a given water lift than Prototype 3.1b.

When the width is changed the oscillation behavior changes. In this case, a $5cm$ increment in width required 4 iterations to the adjustments in the tension of strings, outlet configurations and transversal reinforcement. Since an additional volume is passing trough the ribbons an additional force is exerted over the wood dowels. By increasing the width of the ribbons an additional deflection is expected over the transversal reinforcement and so, a maximum deformation is present in the centerline of the ribbon in the direction of the flow. This deformation changes the way the two polypropylene sheets come together, oscillate and create the pinching point required to lift water, and as consequence, a tuning process is required to achieve maximum flow rate. Fig. 4.20 presents the 4 iterations of this process already mentioned. In the left we can see the variation of the oscillation frequency as a function of the average water flume speed. It can be notice that the tendency for the test $T4.2a$ is unstable since is not represented by a straight line. It must be remembered that this test was conducted immediately after the prototype was constructed. This results demonstrate the necessity to introduce the prototype in water for at least 24 hours to allow the strings to loose their initial rigidity. Test $T4.2b$ shows how, by adjusting the 2 rear transversal reinforcements and allowing the strings to get wet, the oscillation frequency is improved as well as the linear relationship between flume flow speed and oscillation frequency indicating a better uniformity of the oscillation patterns. Even though the oscillation has improved, the flow rate is not at its optimal value. Fig. 4.20 (*right*) shows an unexpected decay for $T4.2b$ in the flow rate at the maximum flume speed. For $T4.2c$ the tension of the 4 rear strings is reduced and as a consequence the oscillation is improved, opposed to the flow rate which does not show an increase. An intermediate tension from those used in $T4.2b$ and $T4.2c$ is used for $T4.2d$, and the results show a reduction of the oscillation frequency with a stable tendency, and an important improvement in the flow rate. This result concluded the process of tuning the prototype and so the configuration is the base to obtain the behavior at different lifting heads h. Similar optimization processes are conducted for prototypes 3.3 and 3.4.

Fig. 4.21 (*left*) presents the stability of this prototype in terms of its oscillation performance. We can see that the frequency at a lifting head $h = 5cm$ is bellow the frequencies at other lifting heads. This is explained by the fact that during the execution of the test at $h = 5cm$ several transversal reinforcements were being adjusted, and due to this, the two last flow rates at this lifting head shown in Fig. 4.21 (*right*) are affected. After these changes were completed an increase in reliability was observed. First, the frequencies remain constant or increase, and second, the transversal reinforcement or strings did not required additional

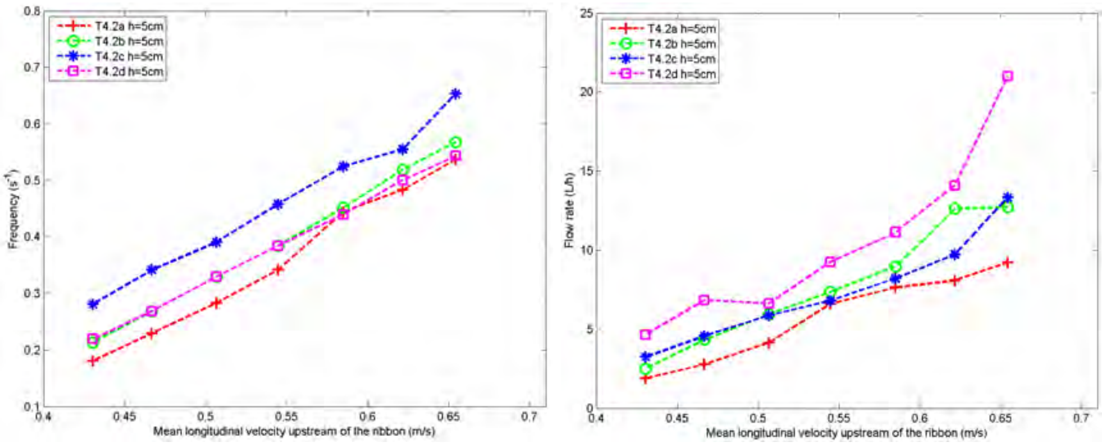

Figure 4.20: Variation of oscillation frequency (*left*), and flow rates (*right*) as function of water speed (u) for Prototype 3.2 under test T4.2a to 4.2d.

adjustments.

Fig. 4.21 (*right*) shows the flow rate that this design pumped at different water lifts (h). As will be seen in Section 4.1.13 and Figure 4.25, Prototype 3.2 performs better than Prototype 3.1b, except for the two highest flume speeds. For example, at a lifting head $h = 5cm$, Prototype 3.2 delivers $21.0L/h$ at an average flume speed of $0.65m/s$ while Prototype 3.1b delivers $20.8L/h$ at the same flume speed. It is considered that in terms of flow rate there is no difference, but it must be remember that Prototype 3.2 was affected at this speed by the release of a transversal reinforcement which affected the final volume of water delivered. This effect can also be seen in the shape of the tendency for $h = 5cm$ in Fig. 4.21 (*right*). While for example $h = 10cm$ presents a gradual variation in slope as the speed increases, the variations for the minimum lifting head $h = 5cm$ present sudden changes with local minimum and maximum. This changes represent the sudden failure of string or wood dowels during the execution of experiments, which usually were corrected after the flow rate was determined at a specific water head and flume speed. It is concluded at this moment that the increase

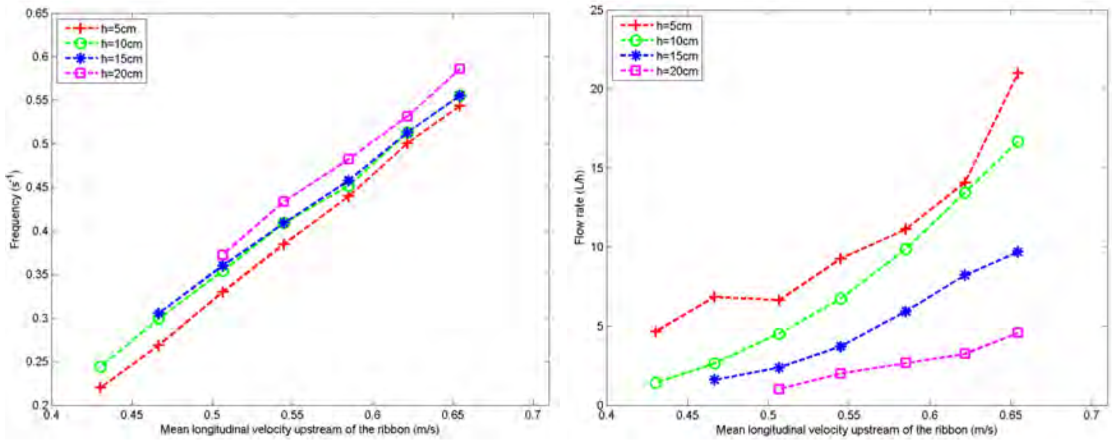

Figure 4.21: Variation of oscillation frequency (*left*), and flow rates (*right*) as function of water speed (u) for Prototype 3.2 under test 4.2d for different water head levels h to be lifted.

of 5cm in the width (W) improves the flow rate delivered compared with a W of 30cm, even if the two highest flow rates at $h = 5cm$ have no difference between Prototypes 3.1b and 3.2.

4.1.11 Prototype 3.3

As described in Table 3.10, Prototype 3.3 has a polypropylene thickness of 0.50mm (0.02in), a 0.00076in (0.019mm) thick internal membrane with a 3mm seal and 2cm of extension , a CPR valve as a check valve, separation between ribbons $\delta = 5mm$, and width W of 40cm. For all water lifts ($h = 5cm$, $h = 10cm$, $h = 15cm$, $h = 20cm$), the frequency of the recirculating pumps (f_{pump}) varied from 22Hz to 34Hz on increments of 2Hz, establishing seven tests per head to be overcame. Prototype 3.3 was successful in oscillating at all of the 28 tests conducted and pumping water at 26 of the 28 tests (the exceptions were the two lowest speeds at $h = 20cm$), showing a better performance than Prototype 3.2 in terms of flow rate and operating range .

As was the case for Prototype 3.2, this design underwent a similar process of optimization. Once the width is changed the oscillation behavior changed. In this case, a width $W = 40cm$ required 3 iterations that suggested adjustments in the tension of strings, outlet configurations and transversal reinforcement. Again, a higher deflection is expected in Prototype 3.3 than the one expected in 3.2. Fig. 4.22 presents the 3 iterations of this process just mentioned. On the left we can see the variation of the oscillation frequency as function of the average water flume speed. It can be noticed that the tendency for test $T4.3a$ is stable in oscillations but lower in frequency compared with the previous tests. In addition, Fig. 4.22 (*right*) shows an unstable tendency in terms of flow rate delivered for test $T4.3a$, indicating that improvements were needed. Visually, this was manifested in the test via deflection in the wood dowels, which was induced by the bulging created in the internal membrane due to the additional volume of water trying to pass through the prototype. After some adjustments were performed in the tension of rear strings and the positioning of transversal reinforcements, tests $T4.3b$ and $T4.3c$ showed stable and almost identical behavior both in terms of oscillation frequency (Fig. 4.22 *left*) and flow rate (Fig. 4.22 *right*).

A final comment is that all the oscillation frequencies from Prototype 3.3 are higher than those that occurred in Prototype 3.2. This means the process of optimization has achieved a better result for the later prototype (if a prototype oscillates better it means more cycles per period and as a result more flow rate delivered). As a consequence, a better flow rate will be delivered not only for the increase in width but also due to the better oscillation.

Fig. 4.23 (*left*) presents the stability of this prototype in terms of its oscillation

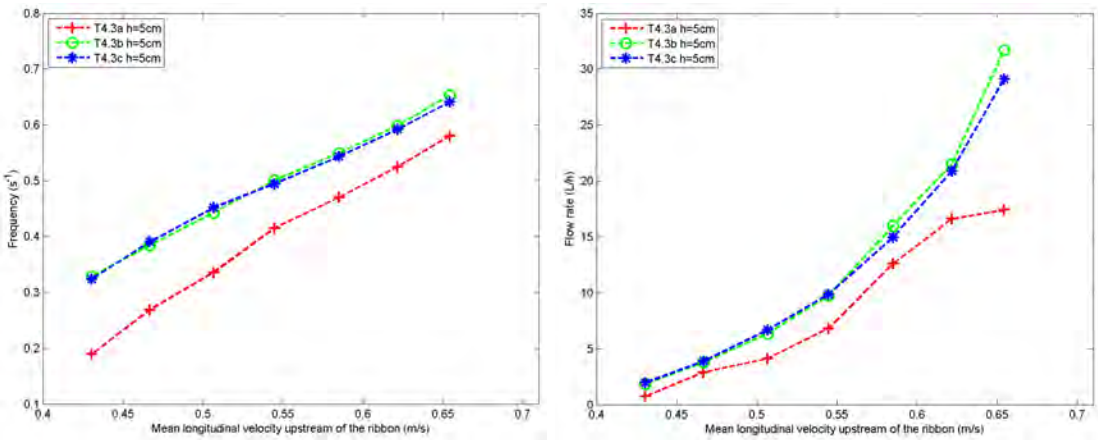

Figure 4.22: Variation of oscillation frequency (*left*), and flow rates (*right*) as function of water speed (u) for Prototype 3.3 under test T4.3a to 4.3c.

performance. We can see that the frequency at any lifting head increases steadily in a linear tendency. This means that both the reliability and the process of optimization have reached an stable value (change in materials or configuration are required in order to obtain a sudden increase in performance). Fig. 4.23 (*right*) shows the flow rate that this design generated at different water lifts (h). As will be seen in Section 4.1.13 and Fig. 4.25, Prototype 3.3 performs better than Prototype 3.2 for all flume speeds and water lifts. For example, at a lifting head $h = 5cm$ Prototype 3.2 delivers $21.0L/h$ at an average flume speed $0.65m/s$ while Prototype 3.3 delivers $29.1L/h$ at the same flume speed.

4.1.12 Prototype 3.4

As described in Table 3.10, Prototype 3.4 has a polypropylene thickness of $0.50mm$ ($0.02in$), a $0.00076in$ ($0.019mm$) thick internal membrane with a $3mm$ seal and $2cm$ of extension , a CPR valve as a check valve, separation between ribbons $\delta = 5mm$, width W of $44cm$ and a separation between steel bars $W_r = 59cm$

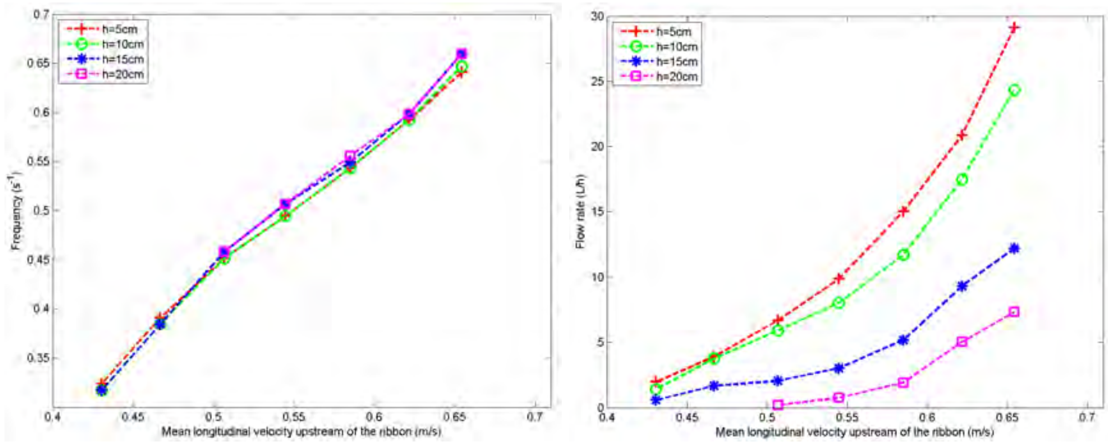

Figure 4.23: Variation of oscillation frequency (*left*), and flow rates (*right*) as function of water speed (u) for Prototype 3.3 under test 4.3c for different water head levels H to be lifted.

($1cm$ less than the expected). The optimization process for Prototype 3.4 was unsuccessful as can be seen in Fig. 4.24. At the left we can see the variation of the oscillation frequency as function of the average water flume speed. It is noticed that an improvement in terms of frequency value was achieved as revealed by the increased slope of the oscillation frequency vs flume speed plots for test $T4.3b$ and $T4.3c$ relative to $T4.3a$. Regardless of this improvement, the flow rate as a function of water speed (Fig. 4.24 *right*) shows that the optimization process did not achieved an optimal value. First, the trend for test $T4.3a$ is unstable, increasing and decreasing its slope suddenly. This means both the tension in the string and the transversal reinforcement were not properly adjusted for this design. Then, the tendencies for test $T4.3b$ and $T4.3c$ are better in terms of how their slope is varying, but still the flow rates delivered and the gradual drop in flow rate for $T4.3c$ at the higher flume flow velocities indicate a problem in reliability.

There are several reasons that help explaining the unfinished optimization of this prototype. First, the difference between the width W and the separation between steel bars W_r is 5cm, 1 cm less than all the prototypes tested before. The spacing of 6cm was chosen since it avoided the influence of the vortices created by the steel frame, provided a proper distance to induce the sine wave, and allow the ribbon to reach certain amplitudes that helped both in the frequency of oscillation and the volume of water delivered. By changing this factor all variables are affected, and as a consequence, the process of optimization followed by the previous prototypes cannot be followed for this specific prototype. On the other hand, if we disregard the fact that one of the variables is different from the other prototypes, we can also argue that the width of the prototype has affected its own performance. The wider the prototype, the more deflection is induced in the transversal reinforcement. As a consequence of this additional deflection, the capacity to oscillate is reduced, and more importantly, the capacity to generate the traveling pinching point in the middle of the prototype is negatively affected. In order to prove the latter hypothesis, all the variables must remain the same, and so, no conclusion is reached about the optimum limit of the width at the moment. Additional tests can be run for wider prototypes in order to find the deflection point where the width starts affecting the flow rate delivered.

4.1.13 The influence of the ribbon's width W in Prototype 3

In order to determine the influence of the width on the flow rate delivered by the prototype, the data from prototypes 3.1b, 3.2 and 3.3 were considered. Each prototype has a width W of $30cm$, $35cm$ and $40cm$, respectively. As explained before, an optimal configuration for Prototype 3.4 was not achieved and as a consequence the data series from this design is not included in the analysis. Fig. 4.25 (*left*) presents the variation of flow rate delivered as a function of water

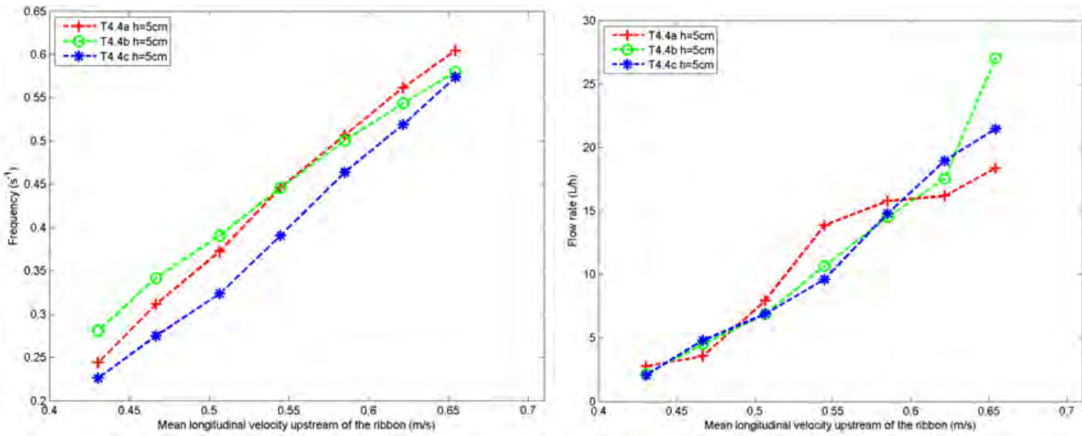

Figure 4.24: Variation of oscillation frequency (*left*), and flow rates (*right*) as function of water speed (u) for Prototype 3.4 under test T4.4a to 4.4c.

speed (u) for the prototypes mentioned above at a lifting head of $h = 5cm$. Prototype 3.2 generates a greater flow rate than Prototype 3.1b except for a flume speed of $0.62m/s$. It is important to remember that the last two data points from the Prototype 3.2 tests were affected by the performance of strings and transversal reinforcements. Regardless of this, Prototype 3.2 performs better than 3.1b, delivering on average $2.6L/h$ more (excluding the last two data points).

Analyzing the performance of Prototype 3.3 in Fig. 4.25 (*left*) we can say that its flow rate did not achieve an optimum value after a flume speed of $0.54m/s$. At the lower flume speeds ($0.43m/s$ and $0.47m/s$) Prototype 3.2 delivers $2.6L/h$ and $2.9L/h$ more than Prototype 3.3. At a flume speed of $0.51m/s$ Prototype 3.3 merely surpasses the former prototype by $0.05L/h$, then the difference starts increasing at $3.9L/h$, then $6.8L/h$ and reaching $8.1L/h$ of difference at the highest flume speed ($0.65m/s$).

Fig. 4.25 (*right*) presents the difference of flow rate delivered between Prototype 3.3 and Prototype 3.2 for all the lifting heads analyzed. A positive value means that Prototype 3.3 performs better than Prototype 3.2. For a lifting head of $h = 5cm$ P3.2 performs better only in the two lowest flume speeds, then P3.3 performs better always and the difference starts increasing. At $h = 10cm$ P3.3 performs better and the difference increases as the flume speed increases, while at $h = 15cm$ and $h = 20$ a clear advantage of P3.3 is only notice at the two highest flume speeds.

Based on the information above, by increasing the width of the ribbon an improvement in flow rate delivered is noticed. Even if we see an increase of an average $2.6L/h$ from $W = 30cm$ to $W = 35cm$, and an increase from $3.9L/h$ to $8.1L/h$ with a change of W from $35cm$ to $40cm$, we do not have enough data to provide an scaling factor that give us the flow rate for an specific width. Furthermore, the inflexion point where the width is affecting the performance of the design, and thus reducing its flow rate, is still to be determined. I hypothesis managed is that at the scaling factor for the flow rate would be close to the ratio of the widths (i.e., we expect the $W = 40cm$ ribbon to generate 33 more flow rate then the $30cm$ wide ribbon). The data suggests that this may be true but is insufficient to verify the hypothesis since the difference between flow rates increased as function of the flume speeds.

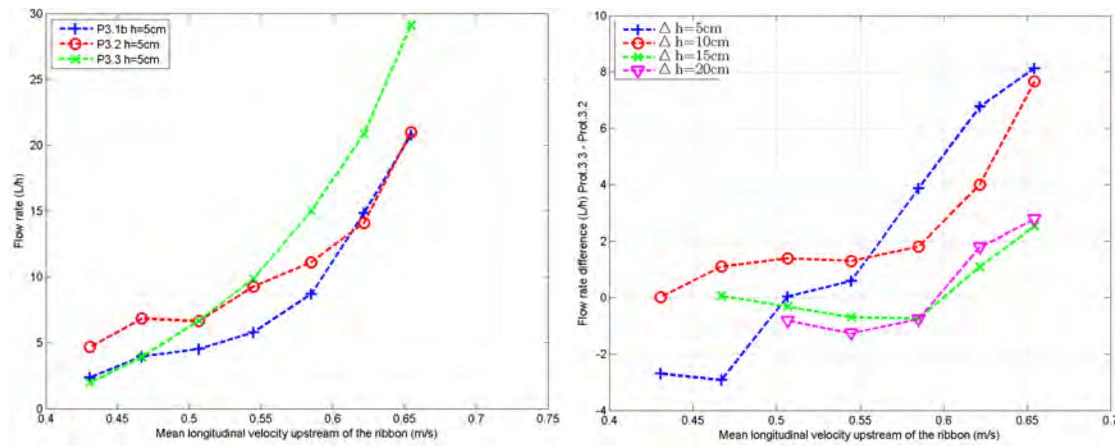

Figure 4.25: Variation of flow-rate pumped as function of water speed (u) for Prototype 3 at $h = 5cm$ (*left*), and difference of flow rate delivered between Prototype 3.3 and Prototype 3.2 (*right*) .

4.2 Characteristic pump curves of the ribbon pump for different configurations

4.2.1 Pump curves for Prototype 2

Fig. 4.26 presents a compilation of the results for Prototype 2 based on the flow rates delivered and the lifting heads h. The figures group the data series by flume speed in order to understand or estimate the possible shut-off head. In the first place, it is important to highlight that the data series corresponding to $h = 5cm$ and $\delta = 10mm$ was not included. The results were affected by sub-optimal pump performance and hence disregarded. As expected, the shut-off head decreases as the δ increases. It was previously explained that by increasing the volume contained between the ribbons, the capacity to oscillate and to generate a pinching point is decreased. As a result of the reduction in performance, we can see in Fig. 4.26 (*down*) that the number of flow rates represented are

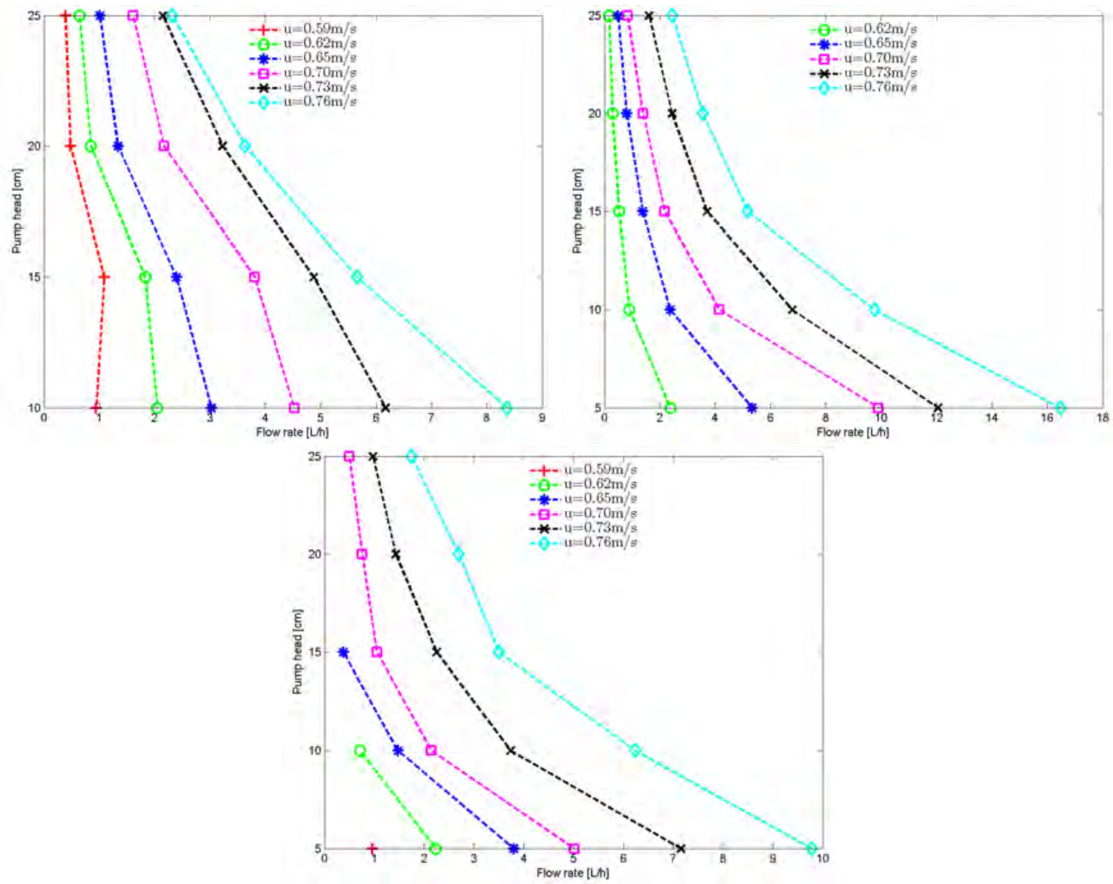

Figure 4.26: Pump curves for Prototype 2 and $\delta = 10m$ (left), $\delta = 20m$ (right) and $\delta = 40m$ (down).

reduced to 1 for $0.59m/s$, 2 for $0.62m/s$ and 3 for $0.65m/s$. It is also evident that the flow rate delivered is bigger as δ decreases, indicating again that the performance and the shut-off head is improved by reducing the space between the ribbons. This is the direct result of a better constriction and a better oscillation.

On the other hand, extrapolations based on spline and quadratic fittings were implemented unsuccessfully to find the shut-off head of each prototype. In the first place there were not enough points in the curve to obtain a good curve fit and second, the fluctuations in the trend of each data set introduced local maximum and minimum values in the interpolations.

4.2.2 Pump curves for Prototype 3

Fig. 4.27 presents a compilation of the results for Prototype 3 based on the flow rates delivered and the lifting heads h. As in Prototype 2, the figures group the data series by flume speed in order to understand or estimate the possible shut-off head. In the first place, it is important to remember that Prototype 3.1b did not delivered a consistent flow rate at a lifting head of $h = 5cm$. Second, Prototype 3.4 was not optimize and as consequence the pump curves are not reported.

The first thing to notice from these two figures is that the flow rate delivered is evidently higher fo Prototype 3.3. This has been seen previously by describing how increasing the ribbon's width increases the volume going trough the prototype. In the same way, when the flume speed is high the tendency of each data series seems to achieve a higher shut-off head as the width increases, but a lower shut-off head for the wider prototypes as the flume speed decreases. A point of inflection seems to exist were the width increases the performance in flow rate but decreases the shut-off head. This hypothesis was not corroborated since, as well as in Prototype 2, the extrapolations were unsuccessful (spline and quadratic fittings were implemented).

4.3 Design, construction and maintenance aspects

The following section presents different aspects encountered during the construction and adaptation of the original design of the Filardo Pump. From design to maintenance different details made the performance of the pump possi-

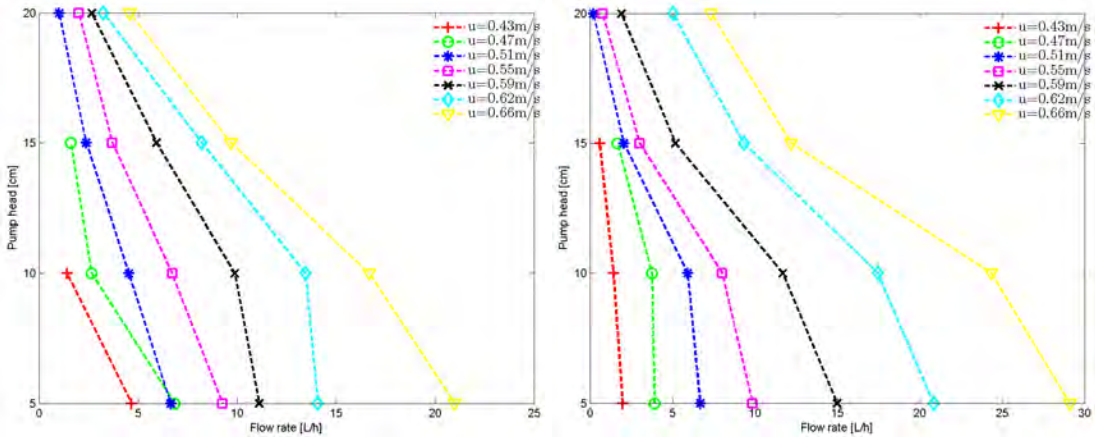

Figure 4.27: Pump curve for Prototype 3.2 (*left*) and Prototype 3.3 (*right*).

ble and as consequence are worth listing. In the same way, the global cost of a device is important information. A detail cost of each component of the modified design is included, as well as the steps for prototype assembly. Finally, an account of the maintenance carried out in the laboratory is presented, and based on those aspects encountered in laboratory settings, an interpretation of possible maintenance aspects in the field are listed.

4.3.1 The design implemented and its variations with respect to the original design

The original design proposed by the inventor was maintained in the following aspects: first, the spacing of the holes in the steel frames, which are the ones that induce the sine wave in the prototype; in the same way, the spacing of holes in the ribbons, which in combination with the spacing in the steel frames lock the deformation in the ribbon; third, the minimum length and width of the prototype (60*cm* by 30*cm*) which was the initial case considered; finally, the separation between the steel frames set as 6 additional centimeters to the original ribbon width.

The following modifications to the design and materials are the result of the iterations followed in this research, and as consequence a product of this study: first, the material of the ribbons (polypropylene) selected for convenience to explore flexibility based on thickness of material; second, the material and design of the internal membrane, featuring a $3mm$ seal and a $2cm$ triangular tail extension comming out of the plastic ribbons; additionally, the implementation of a check valve in general and specifically a CPR valve, its fittings and connection to the internal membrane; moreover, the inclusion of 22 wood dowels of $\phi = 5/16 in$ diameter as transversal reinforcement (11 rods top and 11 bottom); furthermore, the final spacing between ribbons $\delta = 5mm$ which achieved maximum flow rate creating the best seal; in the same way, the mechanism to lock δ through holes perforated in the wood dowels and adjusted and secured with spectra fiber; also, the material (spectra fiber) and final length of the strings locking the deformation of the ribbon; likewise, the inclusion of copper eyelets to prevent the spectra fiber from tearing the plastic ribbons; and finally, the exploration of different ribbon thicknesses and widths.

From the inventor, the original prototype has enough flexibility to operate in vertical or horizontal orientation. The tests run in this investigation were based on the latter and were targeted to avoid surface effects that could influence the oscillation of the ribbon. In the same way, the steel frame is secured from the ground in the original design, opposite to the steel shafts holding the aluminum frame from above in the test conducted in the laboratory. Finally, the ribbons are created to either lift water or harness energy, and this research focused its efforts in exploring the device as a mean to lift water targeting rural areas.

4.3.2 Cost and construction steps

Table 4.4 presents the estimated cost of the materials used to build the prototypes for laboratory testing. A total of USD$31.80 for materials does not include the cost of the aluminum frame and the lateral steel bars. This frame was constructed to fit the specific requirements of the flume that served as a modeled river. For each of the items a 10% TAX and USD$5 dollars of shipping and handling was included as a gross estimate. In terms of the global cost and the possibility to be applied in developing areas the estimation is considered high. Again, it is important to highlight that the major part of this cost comes from shipping and handling, which is expected to be reduced. From the table we can see that the major cost in terms of materials comes from the polyethylene sheets and the CPR valve.

Additionally, Table 4.5 presents each step required to produce a single prototype, again, excluding the process of building the aluminum frame and lateral steel bars. In total 7 hours are required to build the prototype, with the two most time consuming activities being tying the bowline knots into the eyelets and securing the prototype to the steel frame with a total of 160*min*. Also, the drying period of the silicon used in the outlet and the immersion period of the prototype in water are included for an additional 48 hours. On the other hand, an estimated global cost of USD$68.30 is based on a USD$10/hour value. All manufacturing costs are expected to be reduced in the same way as the material costs.

Table 4.4: Materials used in the prototypes, quantity and estimated cost.

Material	Dimensions	Global cost [U$]
Polyethylene sheets	$2 \times 60cm \times 30cm$	9.1
CPR check valve	1	8.8
Dowels rods Birch $\phi = 5/16in$	$22 \times 30cm$	4.8
Copper eyelets $1/8in$ ID	84	4.5
Spectra fiber $\phi = 0.43mm$	$\sim 21.0m$	2.1
Silicon sealant	$\sim 8.5ml$	1.5
Internal membrane	$1 \times 80cm \times 70cm$	0.8
Plastic cable ties	2	0.2
Materials Total		31.8

Finally, it is important to clarify that these are early estimates in both materials and manufacturing time. The primary target must be to increase the efficiency of the device, and parallel to this, reduce the cost of the materials involved in the construction process. This first approximation helps visualizing a global cost of USD$100 without including a sefety factor for either materials or manufacturing, also this estimate is extremely conservative as it does not leverage the cost advantage of making hundreds or thousands of units at a time out of local materials.

4.3.3 Maintenance in the laboratory and in the field

The first aspect of maintenance encountered in the laboratory was the tearing of the strings inducing the deformation in the ribbon. The spectra fiber selected

Table 4.5: Manufacturing process, estimated time and cost.

Activity	Estimated time	Estimated Cost [U$]
Measure and cut Polyethylene sheets	$15min$	2.5
Locate and pierce eyelet	$40min$	6.7
Measure and cut spectra fiber	$30min$	5.0
Tie bowline knots in the eyelets	$70min$	11.7
Measure and cut dowels rods	$15min$	2.5
Locate and drill wholes in the dowels rods	$20min$	3.3
Measure, cut and seal internal membrane	$30min$	5.0
Adjust and secure δ with double external knots and dowel rods	$40min$	6.7
Insert and secure internal membrane in prototype	$20min$	3.3
Secure prototype to the steel frame by tying knots in the head pierced screws	$90min$	15
Lock deformation by adjusting strings	$30min$	5
Secure CPR valve with plastic cable ties and silicon sealant	$10min$	1.7
Drying period of silicon	$24h$	-
Submerge prototype in water to reduce rigidity of spectra fiber	$24h$	-
$Manufacturing\ Total$		68.3

was chosen due to the 80 pounds resistance in tension. However, the failure of these strings was constant. Taking into account that each experiment was run for 5 minutes and each prototype was tested almost 30 times, the reliability of these strings was important. The reason for failure was the shear induced by the constant oscillation of the strings and their contact with the sharp edges of the wholes drilled in the steel bars. Regardless of the attempts for smoothing the edges of these $1mm$ holes, the rupture of the spectra fiber continued in the most tensioned strings (the four front and four rear positions). This situation is not expected to appear on the field. The string will be directly attached to its frame without being inserted into sharp holes.

On the other hand, a similar aspect concerning the strings and the tension induced was the tearing of the plastic ribbons. The polypropylene sheets tend to be torn due to the high tension required to induce the deformation in the four front and four rear positions, and the constant oscillation of the ribbon. This was easily corrected with the introduction of copper grommets in each hole were the spectra fiber is connected.

An additional aspect related to the strings is the possibility to catch debris in the field. This aspect was not analyzed in this research but it is of major importance since the existence of the deformation depends on the tension in the spectra fiber.

The next aspect to take into account is the dowel rods. These parts of the prototypes are responsible for providing transversal reinforcement and to lock the spacing between plastic sheets. In the first place, the force exerted over the rod will not be enough to break the piece, but care must be taken with the deformation since allowing a higher deflection will reduce the performance of the ribbon. A careful selection of this reinforcement must be made, since the material will determine the maximum deformation, and as a result, the quality of the seal that will transport the water down the prototype. Second, the force exerted over the edges of the rods where the strings are holding the spacing (δ) is of the same importance as the deflection. The proper adjustment of this spacing guaranties the existence of the pinching point that will travel downstream of the device. In the laboratory there was no failure of the wood dowels due to the deflection, which is expected to remain constant in the field. However, the strings connecting and securing the spacing δ were subject of constant corrections, and in the same way, this is anticipated to happen on the field. Usually, the strength exerted over the edges of the prototype, which is constantly trying to bulge, is enough to release the wood dowels, eliminating in that way the transversal reinforcement. Additionally, the possibility to catch debris and breaking the rods in the field is also present. This aspect was not analyzed in this research but it is, as well as for the strings, of major importance. The dowel rods are responsible for maintaining the shape of the device and providing the seal that will transport the water downstream. Ultimate we envision the ribbon being manufactured from a local plastic source, ideally recycled plastic, and extruded or cast with lateral stiffeners directly, such as laterally oriented corrugations or some other lateral stiffener.

The next key component is the internal membrane, which required special care in the seals and the connection with the outlet. The membrane was ultimately built with an impulse sealer providing a 3mm seal which performed without errors during the experiments. No additional maintenance was required in this aspect but care must be taken since the laboratory experiments were conducted in clean water. The weakest part of the membrane is the connection with the check valve. The final design included 2 to 3 plastic cable ties and a final seal of silicon sealant. This guaranteed a good performance during the experiments. Nevertheless, this type of connection tends to loose its seal and also, due to the constant oscillation of the prototype, tears the plastic that its holding the check valve. In the field, the degradation of the outlet connection can be improved with the selection of a more resistant material but additional rigidity should not be added. In the same way, clogging and debris are critical aspects to be understood and solved, and again, they were not studied.

Another aspect to take into account is the force exerted over the frame holding the prototype. Apart from the drag force, with each oscillation an additional force is transferred from the prototype to its foundations. When the rear half of the prototype goes up or down a kick shakes the whole structure, requiring in the laboratory four clamps to hold the aluminum frame. It was not possible to quantify this force with the force transducers available in the flume of the DeFrees Hydraulic Laboratory, but its presence is noticeable and the effects on foundations in the field could be either frame rupture or release of the foundations.

Finally, it is possible to say that in terms of maintenance the device is reliable for laboratory settings. It is critical to improve the performance and durability of the internal membrane for the prototype to operate successfully in the field. The ribbons, the strings and its movements are robust enough to operate under real conditions. Even with the presence of debris the oscillation of a field deployed prototype will be constant. In contrast, the internal membrane will suffer constant deterioration affecting the overall performance.

CHAPTER 5

CONCLUSIONS AND RECOMMENDATIONS FOR FUTURE WORK

5.1 Conclusions of the optimization of the ribbon pump

1. We have presented the performance and optimization of a self-powered device, the Filardo Pump, usable for lifting water above the energy line or harnessing energy out of flowing water. We have demonstrated that by combining two plastic sheets (*ribbons*) of the same dimensions, inducing a deformation via strings attached to the sides, locking a space (gap) between the ribbons, and inserting an internal membrane and a check valve, we are able to transport water above the energy grade line of the fluid in which the device is immersed, and in the same way the capability of harnessing energy is also demonstrated. Through direct observation we verified the creation of the pinching points and volumes of water contained between these seals. Once half of the period of the sine wave has passed, both the location of the seals and the volumes of water have traveled downstream. The constant repetition of this process through oscillation guarantees a constant delivery of water synchronized in two motions, which span half a period of the sine wave in the specific case under study.

2. We have verified through the test required to optimized the device that the capacity to oscillate, measured as frequency, is directly proportional to the flow rate delivered. We have also confirmed that the frequency of oscillation depends on the average velocity of the flume, but the value will be affected by the tension applied by the strings, thickness of the plastic sheets, the existence of a transversal reinforcement, and the definition of

an optimum spacing between ribbons (δ).

3. In the same way we have proved that the capacity to lift water above the energy line and the flow rate delivered depends on the tension applied to the strings, the transversal reinforcement, the spacing between the ribbons, and the frequency of oscillation. Regardless of the flume flow rate, if the appropriate conditions are not met, the device will oscillate but will not lift water efficiently.

4. We have documented the reliability and robustness of the prototype. We showed that even with small ruptures in the internal membrane, strings cut, and transversal reinforcement released, the device is able to keep operating and pumping. We theorized that the concept (a permanent unstable induced deformation locked by tension provided by strings on the sides) is robust enough to operate under flows with debris of extreme events. We have also corroborated the importance of the internal membrane and its key role in the reliability of the prototype as a water lifting device. We established the necessity to test new materials that increase the resistance to tear at the same time that add negligible rigidity to the membrane.

5. On the other hand, we established the importance of different components key for the performance of the device. Elements not included in the original design by the inventor such as the check valve, the extension of the internal membrane coming out of the ribbons to connect the valve, the transversal reinforcement and the eyelets, are essential for the prototype to operate as a lifting device. We demonstrated that: first, without a proper check valve there is no possibility to pump water; second, the design of the connection of the check valve with the internal membrane

is critical to guarantee the oscillations. The design of this extension could either enhance or damped the oscillation frequency; third, the transversal reinforcement holds the shape of the device as the water passes through it trying to bulge the internal membrane into a pipe like shape; and finally, the eyelets prevent the plastic ribbons from being torn by the tension and oscillations.

6. In the optimization process we documented the variation of flow rate based on scaling the space between the ribbons, the width and its thickness. In the first place it was demonstrated that a $\delta = 5mm$ is the optimum spacing to achieve maximum flow rate at any width. It was also proved that by increasing the spacing we increase the volume contained between constrictions, but at the same time we affect the performance of these seals reducing the flow rate delivered. Second, we also demonstrated that by increasing the width we increase the flow rate delivered. Due to the changes in behavior in the different prototypes (Prototype 3) we are not able to provide an exact scaling based on the ratio of the increased width. The influence in the shut-off head is also not clear. Third, we confirmed that the only influence of changing the thickness of the ribbon is on the frequency of oscillation. Basically, the linear tendency is shifted and as consequence, a thicker ribbon in a higher flume speed will oscillate at the same frequency as a thinner ribbon in a lower flume speed. The same behavior is expected of a change of material but in this case based on its rigidity. Additionally, we also presented the influence of redesigning the check valve and the internal membrane. We showed that by reducing the minor loss coefficient in the check valve and improving the seals in the internal membrane the flow rate delivered improved. Finally, neither the

influence of the length or the amplitude was studied.

7. Finally, even if we used a flow deep enough to avoid influence of surface effects on the prototype, we corroborated that we only need a flow deep enough to cover the sine wave induce for the prototype to operate. The surface effects will oscillate as the ribbon oscillates, and thus will enhance the frequency (to what extent is to be determined). As a result the minimum depth will be set by the amplitude of the sine wave plus 10 to 15 centimeters to avoid contact either with the bottom or the water surface.

5.2 Recommendations for future work

This project was oriented to prove the ability of the device to pump water and to optimize the design based on geometrical changes. The first recommendation for future works is to understand the flow field surrounding the prototypes, the fluid-structure interaction, and in consequence, the forces driving the motion of the sinusoidal phase. An initial hypothesis is that a combination of viscous and form (pressure) drag on the crest and trough of the sine wave push the deformation downstream. Additionally, a complete description of the flow field will allow an important understanding about the behavior of the pump in a real environment, possible implications, as well as the interaction with wild life and debris.

In terms of the work already performed improvements can be carried out in the understanding of the scaling factor for the width of the device. An important advance is included in this work but the optimal value was not found. Wider prototypes in a wider flume will be of value to understand the influence of this geometrical aspect. In the same way, new studies can also be focused on the improvement of the check valve and the reduction of the minor loss coefficient. Additionally, the author proposes to test an internal membrane featuring 2 or 3 outlets, which will probably reduce the shut-off head but will increase the flow rate delivered.

On the other hand, studies should be conducted to understand the influence of longer ribbons, the influence of more wavelengths in one prototype, and the influence of the amplitude of the induced deformation. Also, work most be done to understand how the forces are transferred to the supporting structure, and with the help of this information, design and build possible supporting frames intended for field use.

Moreover, a great effort is recommended to test the device in the field. In the first instance, it will be important to understand how the prototypes behaves in real flows under the presence of strong secondary currents, changes in stream velocity, debris, and wild life. Second, it will be important to understand the performance and reliability through time, and the requirements of maintenance after long periods of operation.

Finally, a completely different approach could be taken by trying to harness energy. By lifting water above the energy line we have demonstrated the possibility of extracting energy out of the moving fluid is possible. The application of the concept to this purpose remains a subject of competence for future works.

BIBLIOGRAPHY

[1] Brikke, F. (2000). Operation and maintenance of rural water supply and sanitation systems: A training package for managers and planners, Water Sanitation and Health, Netherlands.

[2] Burton, J.D. and Short, T.D. (1999). Induced flow reciprocating pumps., Part 1. Proc. Instn. Mech. Engrs. Part A. Journal of Power and Energy, 213(A5), 363-373.

[3] Cowen, E.A., Tinoco, R.O., Filardo, P., Filardo, F., Shan, B. (2011). Low-cost, sustainable water-powered pump for use in streams and drainage and irrigation channels in rural areas and developing countries. Cornell University technical report.

[4] Cowen, E.A., Tinoco, R.O., Holst-Warhaft, G., Steenhuis, T., Filardo, P., Filardo, F., Shan, B. (2011). Development of a low-cost, robust, sustainable water-powered pump for use in flowing waters. Cornell University technical report.

[5] Departamento Administrativo Nacional de Estadística, DANE (1993). Censo nacional de población y vivienda. DANE, Colombia.

[6] Departamento Administrativo Nacional de Estadística, DANE (2003). Informe de coyuntura económica regional. DANE, Colombia.

[7] Departamento Administrativo Nacional de Estadística, DANE (2005). Censo nacional general 2005. DANE, Colombia.

[8] Efron B, Tibshirani R (1993). An introduction to bootstrap. Chapman and Hall, London.

[9] Tropea, C., Yarin, A. L., and Foss, J.F., (2007). Springer Handbook of Experimental Fluid Mechanics: chapter 23. Springer, Berlin.

[10] Filardo, P. (2010). Pliant or compliant elements for harnessing the forces of moving fluids to transport fluids or generate electricity. US 2010/0078941A1.

[11] Fraenkel, P.L. (1986). Water lifting devices, FAO Irrigation and drainage paper 43. FAO, Rome.

[12] Fraenkel, P. and Thake, J. (2006). Water lifting devices. Practical Action.

[13] Goring, D. G. and Nikora, V. I. (2002). "Despiking acoustic doppler velocimeter data." J. Hydraul. Eng., 1281, 117–126.

[14] Harvey, P. (2007). Handpump Data, Selected Countries in Sub-Saharan Africa Rural Water Supply Network, http://www.watsan.org/docs/2007-data-on-number-of-broken-down-handpumps-in-Africa.pdf.

[15] Howard, G., Bartram, J (2003). Domestic Water Quantity, Service Level and Health. World Health Organization, Geneva.

[16] Kay, M. and Brabben, T. (2000). Treadle pumps for irrigation in Africa, International Programme for Technology and Research in Irrigation and Drainage, FAO, Rome.

[17] Mahkamov, K. and Orda, E.P. (2005). Solar thermal water pumps: A preliminary analysis of the working process. J. Sol. Energy Eng., 127(1), 29-36.

[18] Mori, N., Suzuki, T. and Kakuno, S. (2007). Noise of acoustic Doppler velocimeter data in bubbly flow, Journal of Engineering Mechanics, American Society of Civil Engineers, Vol.133, Issue 1, pp.122-125.

[19] Munson, B.R., Young, D.F., Okiishi, T.H. (2002). Fundamentals of Fluid Mechanics 4th Ed. John Wiley & Sons, New York.

[20] Orda, E.P. and Mahkamov, K. (2004). Development of low-tech solar thermal water pumps for use in developing countries. J. Sol. Energy Eng., 126(2), 768-773.

[21] Pliant Energy Systems (2012). Architecture of Ribbon Frond Pump (Confidential). Pliant Energy Systems, New York.

[22] Pliant Energy Systems (2011). Ribbon Frond Hydrodynamic Behavior (Confidential). Pliant Energy Systems, New York.

[23] World Health Organization and UNICEF (2013). Progress on sanitation and drinking-water - 2013 update , France.

[24] United nations (2012). The Millennium Development Goals Report 2012 (2012). UN, NY.

[25] Tropea, C., Yarin, A. L., and Foss, J.F., (2007). Springer Handbook of Experimental Fluid Mechanics. Springer, Berlin.

[26] Wade, N.S. and Short, T.D. (2007). The performance of a new positive displacement pump targeted to improve rural water supplies, Proceedings of the Institution of Mechanical Engineers, Journal of Power and Energy, 221(8), 1163-1171.

[27] White, F.M. (2011). Fluid Mechanics. McGraw Hill, New York.

[28] Williams, C., Beattie, A., Parker, T., Read, J., and Booker, J.D. (2011). Rope-pump system modeling using renewable power combinations, Proceedings of the World Renewable Energy Congress, Sweden.

[29] International Bank for Reconstruction and Development / The World Bank (2013). World development indicators 2013. World Bank, Washington DC.

[30] Zhang J, Childress S, Libchaber A, Shelley M. (2000). Flexible filaments in a flowing soap film as a model for one-dimensional flags in a two-dimensional wind. Nature, 408(6814): 835-9.